
**PRINCETON UNIVERSITY**
**Department of Chemical Engineering**

# The Design of Optimal Material Combinations for the Membrane Electrode Assembly of a Proton Exchange Membrane Fuel Cell

by Elizabeth Stockton Howard
May 2006
Advisor: Jay B. Benziger

Submitted in partial fulfillment of the requirements for the degree of
Bachelor of Science in Engineering.

Department of Chemical Engineering and
Environmental Studies Certificate Program
Princeton University

This thesis represents my own work in accordance with University regulations.

I authorize Princeton University to lend this thesis to other institutions or individuals for the purpose of scholarly research.

Elizabeth Stockton Howard

I further authorize Princeton University to reproduce this thesis by photocopying or by other means, in total or in part, at the request of other institutions or individuals for the purpose of scholarly research.

Elizabeth Stockton Howard

Princeton University requires the signatures of all persons using or photocopying this thesis. Please sign below and give address and date.

I would like to dedicate this work to my older brother George, my parents, and my peers in the Chemical Engineering department whose positivism, humor, and laid-back attitudes have been the key to my survival through four years in Chemical Engineering at Princeton.

## Acknowledgements

I would like to thank Professor Jay B. Benziger for being my advisor and professor through four years at Princeton, Professor Andrew Bocarsly for supervising my experimental work in the Bocarsly Fuel Cell Laboratory, Paul Majsztrik for his unlimited patience, assistance, and company, Barclay Satterfield and Erin Kimball for their assistance in the Benziger lab, the School of Engineering and Science administrative staff, particularly Dean Bogucki, Vanessa Carter, Sharon Kulik and Hema Ramamurthy, and last but not least, my peers in the Chemical Engineering department for making it all worth it.

## Abstract

Fuel cells efficiently convert fuel (usually hydrogen) directly into DC electricity and are intrinsically nonpolluting. Polymer electrolyte membrane fuel cells incorporate a polymer exchange membrane electrolyte and therefore are lightweight and operate between 60 and 100 $^{0}$C, which makes them ideal candidates for use in automobiles. However, the price of fuel cell materials such as the polymer membrane and the catalyst materials must be reduced and oxygen reduction reaction (ORR) kinetics at the cathode must be facilitated in order to boost fuel cell performance. Platinum, an expensive but common catalyst in polymer electrolyte membrane fuel cells, is highly adsorptive of intermediates and therefore inhibits the already slow ORR. The adsorptive character of platinum alloys is weaker, allowing the ORR rate to increase. Gold, which is less expensive than platinum, lacks adsorptive character but when combined with other metals in alloys does not lead to an increase in catalytic activity compared to platinum. Gold, when combined in an isopropanol slurry with platinum and applied to the surface of the cathode was found to increase the catalytic activity significantly. Mixtures containing various percent weights gold to platinum were tested at four conditions. The best results were obtained at the low temperature, low relative humidity testing condition. Maximum power density increased with weight percent gold, peaked between 40 wt. % gold and 60 wt. % gold, then decreased with further increase in weight percent gold. The 40 wt. % gold cathode catalyst offers as much as a 54% improvement in power density over the platinum cathode catalyst. The 60 wt. % gold cathode catalyst offers as much as a 66% improvement over the platinum cathode catalyst. Although many barriers lie between current energy technologies and a fuel cell powered future, incorporating gold in the catalyst layer at the cathode proves to be a significant step forward.

Table of Contents

# List of Tables

# List of Figures

# I. INTRODUCTION

## A. What Is A Fuel Cell?

A fuel cell acts as a highly efficient and intrinsically nonpolluting electrochemical energy converter that converts the chemical energy of a fuel, usually hydrogen, directly into DC electricity. The many advantages of fuel cells mandate their eventual mass production and cost reduction. The design of fuel cell technology involves components such as available fuels and their processing, the electrochemical processes, especially electrocatalysis, and systems technology for complete fuel cell aggregates including the control of gas, water and heat management. An English physicist, William R. Grove, first invented fuel cell technology in 1839 and found that the electrochemical processes involved take place on the electrode surface at the line where the liquid phase, the gas phase, and the solid platinum catalyst met and, in so doing, opened the inquiry into increasing the efficiency of fuel cells via improvements of the catalyst layer. Although there are currently several types of fuel cells, the polymer electrolyte membrane fuel cell (PEMFC) is most likely to be incorporated in automobiles and offer significant emissions advantages. The primary areas of PEMFC development fall under two categories: the development of a hydrogen infrastructure and the mass production of efficient membrane electrode assemblies. The work presented in this paper focuses on membrane electrode assembly fabrication and the electrocatalysis of the chemical reactions at the electrodes.

Every fuel cell has two electrodes, one positive and one negative, called, respectively, the cathode and the anode and this is where the electricity-producing reactions occur

$H_2 \rightarrow 2H^+ + 2e^-$

**Eq. 1** Reaction at the anode

$\frac{1}{2} O_2 + 2H^+ + 2e^- \rightarrow H_2O$

**Eq. 2** Reaction at the cathode

simultaneously at the three-phase interface discovered by Grove. These electrochemical reactions are:

The overall reaction is the oxidation of hydrogen to produce water:

$$H_2 + ½\ O_2 \rightarrow H_2O$$

**Eq. 3** Overall fuel cell reaction

Hydrogen atoms enter a fuel cell at the anode and are adsorbed on the anode where a chemical reaction strips them of their electrons resulting in protons. The protons move through an electrolyte, which acts as an ionic conductor, under a chemical potential gradient from the anode to the cathode. The negatively charged electrons move through an external circuit, providing the current through the wires to do work. Oxygen enters the fuel cell at the cathode and, in some cell types, it combines with the electrons returning from the electrical circuit and the hydrogen ions that have traveled through the electrolyte from the anode. Every fuel cell also has an electrolyte, which carries electrically charged particles from one electrode to the other, and a catalyst, which speeds up the reactions at the electrodes. Hydrogen is typically the fuel but fuel cells also require oxygen. One important advantage of fuel cells is their ability to generate electricity with very little pollution – most of the hydrogen and oxygen used in generating electricity combine to form a harmless byproduct, water. Although a single fuel cell generates a small amount of direct current (DC) electricity, more than one fuel cell may be assembled into a stack to create more current.

Because the overall reaction in a hydrogen fuel cell is the same as the reaction of hydrogen combustion, the heat of the reaction is the same as the enthalpy (or heating value) of hydrogen and the thermodynamics of fuel cells can be derived from this value. The combustion of hydrogen is an exothermic reaction, releasing 286 kJ/mol at 25 $^0$C,

which is equivalent to saying that the enthalpy of hydrogen is –286 kJ/mol at 25 $^0$C. This heating value is a measure of the energy input in a fuel cell. It is the maximum amount of thermal energy that may be extracted from hydrogen. However, not all of this energy can be converted into electricity because a portion of the energy is converted into entropy. The portion that can be converted into electricity is known as the Gibbs free energy and is equivalent to 237.34 kJ/mol at 25 $^0$C. The remaining 48.68 kJ/mol is converted into heat. Using the mathematical expression for work, an expression can be derived that relates the theoretical potential for fuel cells to the Gibbs free energy. The theoretical potential of a fuel cell is 1.23 Volts at 25 $^0$C.[i] An increase in cell temperature results in a lower theoretical cell potential. However, at higher currents in operating fuel cells, a higher cell temperature results in a higher cell potential because the voltage losses in operating fuel cells decrease with temperature and this more than compensates for the loss of theoretical cell potential. As the current approaches zero, the voltage is larger at lower temperatures and does not increase with an increase in temperature. If a fuel cell is supplied with reactant gases but the electrical circuit is open, it will not generate any current and the cell potential is expected to be at, or at least close to, the theoretical cell potential for the given conditions (temperature, pressure, and concentration of reactants). This is known as the *open circuit potential* and is significantly lower than the theoretical potential – usually less than 1 volt. Voltage losses can be attributed to the following factors: kinetics of electrochemical reactions, internal electrical and ionic resistance, difficulties in getting the reactants to reaction sites, internal (stray) currents, and crossover of reactants.[ii] [iii]The purpose of fuel cell technology development is to mitigate these voltage losses and increase the practical, or operating, efficiency of the fuel cell.

## B. Advantages

Fuel cells have many important advantages that necessitate their mass production and cost reduction. These advantages fall under two broad categories: the high theoretical energy conversion efficiency and a potential for sharp reduction of power source emissions. The theoretical Carnot efficiency can be calculated using Equation 4.[iv]

$$\textbf{Eq. 4}\ \eta_{Carnot} = \frac{W}{\Delta H} = \frac{T_1 - T_2}{T_1} = 1 - \frac{T_2}{T_1}$$

However, fuel cells do not underlie the limitations of the thermodynamic Carnot cycle. The theoretical conversion efficiency for a fuel cell directly converting hydrogen to electric power at operation temperatures typical for a polymer electrolyte fuel cell (30 $^0$C – 100 $^0$C) is therefore far greater than that of a heat engine such as an internal combustion engine. The theoretical conversion efficiency for direct fuel conversion is equivalent to the ratio between the useful energy output (the electrical energy produced) and the energy input (the enthalpy of hydrogen). The enthalpy of hydrogen is equal to –286 kJ/mol (at 25 $^0$C). The portion that can be converted into electricity is the Gibbs free energy ($\Delta G = \Delta H - T\Delta S$). The ratio between the Gibbs free energy and the enthalpy of hydrogen gives a theoretical efficiency of 83%. Whereas the ideal or maximum efficiency of an electrochemical energy converter depends upon electrochemical thermodynamics, the real efficiency depends on electrode kinetics.[v] The practical energy conversion efficiency of a fuel cell system, which usually consists of the cell stack, fuel and air supply system,

water and heat extraction system, cooling system, and the control unit, ranges between 35 and 70% even at temperatures under 100 $^0$C. The practical energy conversion efficiency of heat engines is well below 30% and approaches 50% only for large turbines operating at much higher temperatures. Fuel cells operating at or near ambient temperatures at higher efficiencies (or power per weight) are important for mobile applications and since power is the rate of producing energy, the kinetics of the electricity-producing interfacial charge-transfer reactions (electrode kinetics) are important as well.[vi]

The simplicity of fuel cells is also an important advantage over heat engines. The layers of repetitive components that comprise fuel cells and the lack of any moving parts indicate the potential for mass production of fuel cells at a cost comparable to that of existing energy conversion technologies or even lower.[vii] The lack of moving parts also promises a long operational lifespan for fuel cell units. Furthermore, the fact that fuel cells are modular – more power may be generated simply by adding more cells – indicates that mass produced fuel cells may be significantly less expensive than traditional power plants. As opposed to some heat engines, fuel cells are quiet. Their size and weight also make them particularly convenient for a wide variety of applications.

In addition to the energy efficiency and simplicity of fuel cell technology, there also exists a potential for lowering or eliminating altogether hazardous emissions and reducing greenhouse gas emissions. $CO_2$ emissions could be lowered according to the ratio of efficiencies of combustion and electrochemical conversions of fuel energy, which could mean a potential drop in $CO_2$ emissions by as much as 50% per mile driven.[viii] There is no nitrogen oxide (a major pollutant emitted by internal combustion engines) generated by a fuel cell because of the much lower temperature than that of an internal

combustion engine. Other hazardous emissions (e.g. carbon monoxide) are also drastically lower in a fuel cell powered vehicle and are brought to zero when hydrogen is used as the fuel for a polymer electrolyte membrane fuel cell (PEMFC). In this case, water vapor becomes the only exhaust and hydrogen fuel cell vehicles are therefore known as true "zero emission vehicles". For fuel cell vehicles that do not use pure hydrogen as a fuel but instead have an onboard reformer, tailpipe emissions are projected to be a small fraction of emissions from internal combustion engine technologies. Although it is important to consider the full fuel cycle in evaluating fuel cell vehicles with onboard reformers, it is still possible to reduce full fuel greenhouse gas emissions by as much as 50% and lower emissions of other criteria air pollutants such as CO, VOCs, NOx, SOx, and particulates with gasoline or diesel internal combustion engine hybrids compared to today's gasoline cars.[ix] Fuel cell vehicles can have even lower full fuel cycle emissions than internal combustion engine hybrids, depending on the fuel and primary energy source.

### C. Hydrogen as a Fuel

Fuel cell vehicles using hydrogen potentially offer the lowest full fuel cycle emissions of any alternative and also the widest range of primary supply options.[x] Hydrogen is the best long-term option for fuel cell vehicles not only because of its environmental and energy supply benefits but also in terms of vehicle first cost and lifecycle costs. However, the necessary refueling infrastructure is extremely daunting and costly for hydrogen as opposed to liquid fuels. The availability of onboard hydrogen storage systems that are compact and available at low cost is also an issue. The onboard storage problem stems from several chemical properties of hydrogen. Hydrogen has a high heat of combustion

(120 MJ/kg), which is nearly three times higher than the comparable values for gasoline and diesel, and also has a very low density. The energy content of hydrogen is only 9MJ/l. The necessary onboard storage volume for hydrogen therefore has to be larger than for conventional fuels. However, the wealth of options for sources of hydrogen mandate the development of onboard storage, despite the difficulties involved with such storage systems.

There are two different possibilities for providing hydrogen to a fuel cell within a vehicle: onboard reformers and hydrogen production outside the vehicle. Small-scale onboard reformers could be integrated as components of the fuel cell system. In particular, natural gas reformers could be coupled with phosphoric acid or proton exchange membrane fuel cell cogeneration systems. Onboard fuel processors could be used to process methanol or gasoline, producing hydrogen for the fuel cell. Although these reformers are typically designed to produce a reformate gas containing 40-70% hydrogen, they could be adapted to include purification stages to produce pure hydrogen. Reforming can also take place outside the vehicle. In this case, a variety of hydrogen sources could be utilized but the hydrogen would have to be transported to a refueling station and an infrastructure would have to be developed to accommodate for such refueling stations. Onboard fuel processors offer a possible transition to a more complicated, national hydrogen infrastructure.

Methanol reforming seems to be one of the more promising alternatives in terms of building a hydrogen infrastructure. With the correct catalyst, methanol can be converted into a hydrogen-rich stream via steam reforming with water (see Eq. 5) at temperatures as

**Eq. 5** $CH_3OH + H_2O \rightarrow CO_2 + 3H_2$

low as 200 $^0$C, which is much lower than the temperatures required for liquid or gaseous hydrocarbons such as gasoline.

At modest pressures the equilibrium conversion is high (above 99%) and the tendency to form unwanted byproducts is low. The methanol reforming reaction is endothermic and no other liquid fuel, not even ethanol, can be catalytically converted to yield hydrogen at as low a temperature as methanol. The main problems with methanol involve availability and special handling requirements. Although methanol might provide an easy transition from gasoline-powered vehicles to fuel cell powered vehicles, it would necessarily imply an extra fuel in the transition process. Other options for building a hydrogen infrastructure involve transitioning directly from gasoline fuel processors to fuel cell cars or using hydrogen refueling stations first in centrally refueled fleets and then moving to general automotive markets.

If onboard reformers are not utilized in fuel cell vehicles then the hydrogen must be produced elsewhere and piped or carried via truck to refueling stations. Fossil feed stocks such as natural gas or coal may offer the lowest hydrogen costs in many locations, with local contributions from electrolysis powered by low cost hydropower, while at the same time reducing dependence on foreign petroleum supplies. If fuel decarbonization and/or carbon sequestration is pursued it is possible that fossil fuels could be used for transportation with near zero emissions of carbon to the atmosphere.[xi] Currently, over 90% of hydrogen is made thermochemically by processing hydrocarbons in high temperature chemical reactors to make a synthetic gas ("syngas"), which is comprised of hydrogen, CO, $CO_2$, $H_2O$, and $CH_4$.[xii] Syngas is further processed to increase the hydrogen content and pure hydrogen is separated out of the mixture.

Another option for hydrogen production is the use of renewable resources such as wastes, biomass, solar power, or wind power. Solar and wind power in particular could be used for electrolytic hydrogen production, which could meet the projected global demand for fuel. However, the delivered cost for such methods is projected to be about two to three times that for hydrogen from natural gas reformation.[xiii] Where low cost, renewable source electricity is available; water electrolysis is used to produce hydrogen. In this process, electricity is passed through a conducting aqueous electrolyte, breaking water down into hydrogen and oxygen. The hydrogen can then be compressed and stored for later use. If solar or wind power is incorporated and a dense electricity grid with sufficient capacity exists, the most efficient way to supply the energy to the user is electricity. However, if the grid does not possess any spare capacities, the energy can be converted into hydrogen via electrolysis– a storable form of energy – offering up a viable, fuel cell-based solution for the problem of incorporating renewable power sources into the current grid system.

Once produced, hydrogen can be stored as a compressed gas, cryogenic liquid, or in a compound such as a metal hydride or ammonia. The use of hydrogen as an automotive fuel requires storage systems that have inherent safety as well as volumetric and gravimetric efficiency. Traditional storage of hydrogen in metallic pressure vessels leads to low gravimetric efficiency but composite pressure vessels in combination with increased working pressure up to 700 bar achieve high volumetric and gravimetric efficiency. This technology is well known in automotive applications because it is already used in compressed natural gas vessels. Cryogenic storage involves liquefying hydrogen at low temperatures (-253 $^{0}$C) and leads to high volumetric and gravimetric

efficiency. However, it is extremely difficult to handle hydrogen as a cryogenic liquid at this low of a temperature and there is a high amount of energy needed to liquefy hydrogen compared to the storage of compressed hydrogen. Cryogenic storage requires suitable, safe, and reliable storage and filling facilities and especially safe and easy handling of filling equipment comparable to conventional gas stations.

The technical feasibility of hydrogen storage in metal hydrides is controlled by the kinetics of hydriding and dehydriding. There are two possible types of metal hydride storage: storing hydrogen atoms in certain metals ("metallic sponges") that will reversibly hydride and dehydride by the simple gas-solid chemical reaction or the use of certain previously synthesized hydrides ("chemical hydrides") that can be destructively reacted with water to liberate the hydrogen gas. The other option for hydrogen storage is anhydrous ammonia, which has low toxicity, low flammability, and assured purity that results from the method of manufacturing. This option offers significant advantages in cost and convenience due to ammonia's higher density and easier storage and distribution. The heating value of ammonia is similar to that of methanol and ammonia contains 1.7 times as much hydrogen per volume as liquid hydrogen. Furthermore, the cracking process is thermally efficient and simple. Nitrogen generated can be released to the atmosphere without significant local environmental impact.[xiv] However, the development of hydrogen sources and storage technologies is only one vital component of advancing fuel cell technology to the point of mass production, cost reduction, and wide scale implementation.

## D. Types of Fuel Cells

Not only are there various types of hydrogen sources and storage technologies but there are also several different types of fuel cells that have been developed since the basic technology was invented by William Grove in 1839. Not all of these fuel cells offer the same advantages mentioned earlier. The fundamental difference between the different types of fuel cells is the electrolyte material, which affects the operating temperature of the fuel cell and hence, the relevant advantages. At the high range of operating temperatures are molten carbonate fuel cells and solid oxide fuel cells. Molten carbonate fuel cells contain an electrolyte composed of a combination of alkali carbonates, retained in a ceramic matrix of $LiAlO_2$. These carbonates form a highly conductive molten salt and the carbonate ions provide ionic conduction. These fuel cells are inconvenient because of their high operating temperatures (600-700 $^0$C) and are thought to be limited to stationary power generation. However, one benefit is that at this high of an operating temperature, noble metal catalysts are typically not required. Solid oxide fuel cells use a solid, nonporous metal oxide as the electrolyte and operate at even higher temperatures than the molten carbonate fuel cell (800-1000 $^0$C). At high temperatures such as these ionic conduction by oxygen ions takes place.

Alkaline fuel cells, phosphoric acid fuel cells (PAFCs), and polymer exchange membrane fuel cells (PEMFCs) operate at the low end of the operational fuel cell temperature range. Alkaline fuel cells use a concentrated, 85 weight percent, potassium hydroxide (KOH) as the electrolyte for high temperature operation (250 $^0$C) and less concentrated, 35-50 wt %, for lower temperature operation (<120 $^0$C). This potassium hydroxide electrolyte is retained in a matrix (usually asbestos). A wide range of

electrocatalysts can be used. An important drawback of the alkaline fuel cell is that this type of fuel cell is intolerant of $CO_2$ in either the fuel or the oxidant. Phosphoric acid fuel cells (PAFCs) employ concentrated (~100 weight percent) phosphoric acid as the electrolyte, which is contained in an SiC matrix under operational temperatures of 150-220 $^0$C. The electrocatalyst used in PAFCs is platinum. PAFCs are currently semi-commercially available in container packages (200 kW) for stationary electricity generation. PEMFCs utilize a thin (<50 μm) proton conductive polymer membrane as the electrolyte. The catalyst is typically platinum supported on carbon with loadings of about 0.3 mg/cm$^2$, or, if the hydrogen feed contains minute amounts of CO, the catalyst is a platinum-ruthenium alloy.[xv] The optimal operating temperature of PEMFCs is between 60 and 100 $^0$C. Because of this low operating temperature, PEMFCs are a serious candidate for automotive applications and also for small-scale distributed stationary power generation and portable power applications. Due to PEMFCs potential to be used in automobiles and therefore provide the emissions advantages described above, they are the focus of the work presented in this paper.

### E. PEMFCs

Although transportation and off-grid power generation have been emphasized in recent years as the main applications of PEMFCs and solid oxide fuel cells, it is important to note the potential for other applications of PEMFCs. There is currently a considerable need for power sources with energy densities exceeding that of secondary lithium batteries. This need is driven by the consumer electronics industry, which has flourished in the last decade alone. In addition to the emissions advantages that PEMFCs offer to the transportation industry, PEMFCs may be required to power both present and

next generation hand held devices – particularly those that require longer use times per recharge. This opportunity may provide the first market entry for low temperature fuel cells like the PEMFCs discussed in this paper. From an environmental standpoint, PEMFCs offer emissions advantages that compare favorably with current internal combustion engines and also have the flexibility and convenience of being incorporated in automobile designs. With significant increases in efficiency and subsequently lower production prices, portable power systems of superior energy density and immediate refuelability such as the PEMFC could compete with the costs of present battery technology. Current costs of PEM fuel cells range between $1500 and $10,000 per kW, which is two orders of magnitude higher than today's engine technologies.[xvi] If PEMFCs can be mass-produced, their cost could be lowered enough to compete with internal combustion engines as well as present battery technology.

PEMFC technology, invented at General Electric in the early 1960s by Thomas Grubb and Leonard Niedrach, was first introduced as part of the Gemini space program in the 1960s but was considered fundamentally impractical for any terrestrial application as late as the mid-1980s. In the Gemini space program, early PEMFCs used highly pure, cryogenic hydrogen and oxygen and very high precious metal loadings. These high-priced materials were fully acceptable for use in power sources installed in a space vehicle but prohibited the wide-scale implementation of PEMFC technology in other applications. Terrestrial applications demanded lower precious metal loadings, diluted or impure hydrogen as fuel, and air rather than oxygen. Water redistribution in the ionomeric, polymer membranes was also a consideration for terrestrial applications. Technical breakthroughs during the years 1985 through 1995 included the development

of membrane electrode assemblies (MEAs) using precious metal loadings lower by more than an order of magnitude, effective approaches to operation with air and impure hydrogen fuel, and resolution of the water management issues by using a thinner polyperfluorocarbon sulfonic acid membrane. During this time period, power densities approaching 1 kW/liter in prototype stacks were demonstrated. Contemporaneously, public and industrial interest in environmentally sound power sources resulted in an increase in the investment in PEMFC technology by three orders of magnitude.[xvii]

As mentioned before, PEMFCs utilize a polymer membrane electrolyte, which is impermeable to gases but conducts protons, squeezed between two porous, electrically conductive electrodes. The electrodes are typically made out of carbon cloth or carbon fiber paper. The electrodes must be porous because the reactant gases are fed from the back of the electrodes and must reach the interface between the electrodes and the membrane. At the interface between the porous electrode and the polymer membrane electrolyte there is a layer with catalyst particles, which are typically platinum supported on carbon. The electrochemical reactions take place in these catalyst layers, on the catalyst surface. The polymer membrane electrolyte, porous electrodes, and precious metal catalyst comprise the membrane electrode assembly (MEA), which is sandwiched between collector/separator plates. These plates collect and conduct electrical current, provide pathways for the flow of reactant gases (flow fields), and provide structural rigidity. In multicell configurations, the collector/separator plates separate gases in adjacent cells and physically and electrically connect the cathode of one cell to the anode of the adjacent cell.

Within the PEMFC hardware described above, several processes take place, which must be optimized in order for the fuel cell to operate efficiently. The reactant gases must flow through the flow channels – convective flows may be induced in the porous layers. These gases must then diffuse through the porous media and participate in electrochemical reactions, including intermediary steps, at the surface of the catalyst at the interface between the gas diffusion layer and the membrane. Hydrogen, fed on one side of the membrane, splits into its primary constituents – protons and electrons. The resulting protons are then transported through the proton-conductive polymer membrane and the resulting electrical current is conducted through the electrically conductive electrodes, through current collectors, and through the outside circuit where they perform useful work and come back to the other side of the membrane. (See Figure 1 for a schematic of the PEMFC hardware[xviii]). At the catalyst sites between the membrane and the other electrode, electrons meet with the protons that went through the membrane along with the oxygen that is fed on that side of the membrane, resulting in

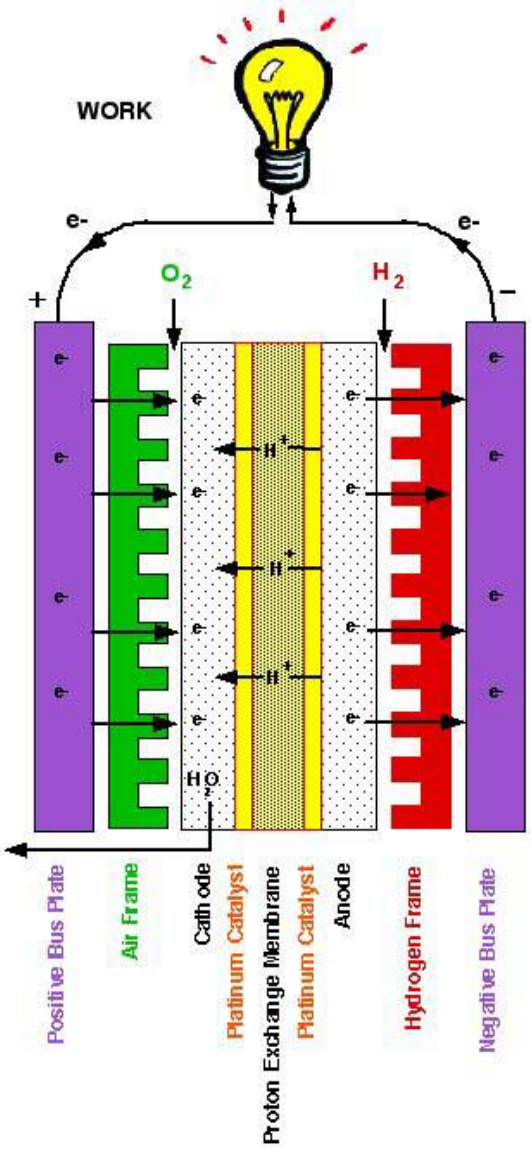

the creation of water in an electrochemical reaction. This product water is transported through the polymer membrane, involving both electrochemical drag and back diffusion. Product water (vapor and liquid) is also transported through the porous catalyst layer and the gas diffusion layers and ultimately pushed out of the cell with excess flow of oxygen. Heat is transferred via conduction through the solid components of the cell and convection to the reactant gases and cooling medium. The net result is a current of electrons through an external circuit.

The potential advantages of fuel cell technology are numerous and hard to ignore in light of shifting energy policies. On a larger scale, demand for hydrogen infrastructure has captured the interest of policy-makers and scientists alike and led to many important developments in this area. Various types of fuel cells can be utilized for a wide range of applications – from stationary power sources to portable handheld devices to vehicles. In particular, the flexibility and low emissions of PEMFCs have begun to spark further interest in the development of fuel cell technology. Due to their low operational temperature and flexibility with regard to fuel and oxidant, PEMFCs are a likely choice for all types of applications. Used with pure hydrogen as a fuel, PEMFCs could power zero-emission vehicles. However, the wide scale utilization of PEMFC technology demands cost reduction, which will only become a possibility if the technology is mass-produced. Likewise, mass production will only become a possibility with significant cost reduction. It is therefore crucial for PEMFC technology, and in particular the MEA technology, to be perfected to the point of increasing the practical efficiency as well as for the fabrication process itself to be made more efficient.

**Figure 1. PEMFC Schematic**

## II. BACKGROUND

"Although PEMFCs have high power density, their open circuit voltage is about 1 V. The theoretical thermodynamic voltage is about 1.2 V. The slow kinetics of the oxygen reduction reaction as well as the hydrogen crossover through membrane are responsible for this difference."

– K. Ota and S. Mitsushima, *$O_2$ reduction on the Pt/polymerelectrolyte interface*

### A. Membrane Electrode Assemblies

The membrane electrode assembly of a polymer electrolyte membrane fuel cell is the fundamental component of the fuel cell technology and it is through design improvements of the membrane electrode assembly ("MEA") that overall efficiency can be brought closer to the theoretical energy conversion efficiency of hydrogen combustion. The MEA is composed of the polymer exchange membrane, sandwiched between two electrodes (typically of carbon cloth or carbon paper), which each have a gas diffusion layer and a catalyst layer that face the membrane. This membrane-electrode sandwich is typically contained within two layers of gasket material that allow the membrane and electrodes to be held in place between the bipolar plates. Although the polymer membrane component has only been recently developed, the gas diffusion layer and catalyst layer concepts were first conceived of by William Grove and his contemporaries in the nineteenth century. The membrane can be any single-ion conducting polymer but perfluorinated ionomer membranes have been found to yield the best operational efficiencies. The membrane known by the trade name Nafion, which is used in the work presented in this paper, was first successfully implemented in the mid-1960s. The fuel cell electrodes are essentially thin catalyst layers pressed between the ionomer membrane and a porous, electrically conductive substrate such as carbon cloth or paper. Typically, carbon supported platinum catalysts and platinum-alloy catalysts are used for proton exchange membrane fuel cells. By increasing the efficiency of the MEA

components it is possible to decrease the platinum loadings and decrease the overall cost of production. With simplification of the MEA production process, mass production of PEMFCs becomes a more realistic goal.

### B. Polymer Electrolyte Membranes

The polymer electrolyte membrane ("PEM") constitutes the basis of the MEA, the performance of which determines crucially the overall power density of a fuel cell system. The PEM's primary function is as the electrolyte through which protons move to conduct ionic current. However, the PEM also acts as a separator between the two gas compartments: the anode and cathode gas compartments, and as the support of the anode and cathode catalyst layers. Single-ion conducting polymer electrolytes give electrochemists the ability to choose from a variety of polymers with both high conductivity for a given ion of interest as well as stability and ability to be processed so as to allow for the ideal design of various electrochemical devices. "Electrochemical separator membranes with fixed ion groups" date back to before the 1950s with the use of polystyrene sulfonic acid and related acid-containing polymers as separators for electrochemical processes. Formerly, sulfuric acid and potassium hydroxide were used as electrolytes because of their low cost and high ionic conductivity but they were found to be extremely corrosive and a challenge to confine. The advantages of these early acid-containing polymers included the lack of corrosive mobile acids and bases, a high conductivity and selectivity, and a thin film form leading to compact systems with low ohmic drop. However, there was excessive chemical and electrochemical degradation that occurred with the instability of the carbon-hydrogen bonds in these early membranes.

The concept of ion exchange membranes as the sole electrolyte in fuel cells with gaseous feed streams was not invented until 1955. In 1962, it was discovered that humidified feed gases improved the performance of membrane fuel cells. In 1966, the first Nafion membrane was used in a fuel cell successfully by GE for NASA. Three years later, DuPont announced the availability of a new XR perfluorosulfonic acid copolymer composition suitable for use in PEMFCs.[xix] The perfluorinated ionomer membranes, which came to be known under the trade names of Nafion membranes and Nafion solutions, are a subclass of the early polymer electrolytes. The term ionomer refers to single-ion conducting polymers with a fixed ion group covalently attached to a side chain of the polymers. A perfluorocarbon-sulfonic acid ionomer is a copolymer of tetrafluorethylene (TFE) and various perfluorosulfonate monomers. Nafion is comprised of perfluoro-sulfonylfluoride ethyl-propyl-vinyl ether (PSEPVE). Nafion membranes are available from DuPont and assigned numbers such as NE112, NE-1135, N115, and N117. The first two digits represent the equivalent weight divided by 100 whereas the last digits refer to how many mils ($^{1}/_{1000}$ of an inch) thick the membrane is. In Nafion, the $SO_3H$ group is ionically bonded and the end of the side chain is an $SO_3^-$ ion with an $H^+$ ion. The ends of the side chains cluster within the overall structure of the membrane. The Teflon-like backbone is hydrophobic and the sulphonic acid at the end of the side chain is highly hydrophyllic. The PTFE backbones provide structural and thermal stability of the membrane and immobilize the dissociated sulfonic acid groups. The hydrophyllic regions are therefore created around clusters of sulphonated side chains. The relative hydrophobicity and hydrophyllicity of the membrane contribute to the advantages, disadvantages, and design considerations.

Despite the high cost of Nafion membranes and concerns about long-term stability of polymers in electrochemical cells due to fears of oxidation damage, Nafion has been found to have favorable chemical, mechanical, and thermal properties along with high proton conductivity when sufficiently hydrated.[xx] In fact, Nafion requires water for proton conductivity and the operating temperature is therefore limited to below the boiling point of water.[xxi] Both the fuel and the oxidant for a PEMFC must be saturated with water vapor. If they are not saturated with water vapor, the water content of the Nafion electrolyte alone is not enough to sustain desirable fuel cell performance. Lack of water decreases the ionic conductivity of the membrane, which causes an increase in the cell's internal resistance. The electroosmotic drag of water from the cell anode to the cell cathode, which accompanies proton transport during fuel cell transport at high current densities, leads to dehydration near the anode and flooding of the cathode with liquid water.[xxii] This lower water content on the anode side of the cell results in an even further reduction in the electrolyte's ionic conductivity. There is a definite correlation between the transport of protons and water to the hydrated morphology of the sulfonic acid-based ionomers. The extremely high hydrophillicity of the sulfonic acid functional groups when combined with the equally high hydrophobicity of the polytetrafluoroethylene (PTFE) backbone results in a two-phase system consisting of a network of water containing domains separated from the PTFE medium.[xxiii] Within the electrodes, loss of water decreases both the electrolyte conductivity and the gaseous reactant permeability. Furthermore, the kinetics of the oxygen reduction reaction are slowed by the loss of water, which results in an increase in the electrode polarizations.[xxiv] By carefully

managing the hydration and water removal of the fuel cell system it is possible to maximize the efficiency with which the fuel cell operates.

Although reaction kinetics of the oxygen reduction reaction at the cathode of a polymer exchange membrane fuel cell are extremely slow, it has been shown that the solid state perfluorinated acid electrolyte environment offers significant advantages over phosphoric acid for oxygen reduction. This is because the perfluorinated acid environment yields higher oxygen solubility and diffusion coefficient. There is also significantly less anion adsorption from the electrolyte. The low temperature operation and relatively hydrated environment of the perfluorinated acid electrolyte leads to a higher degree of water activation and formation of Pt-OH species on the Pt surface. This low temperature operation also leads to different oxygen-reduction reaction kinetics. Furthermore, the hydrated nature of the electrolyte leads to higher proton conduction.[xxv] Each one of these advantages highlights the solid state perfluorinated acid electrolyte's ability to facilitate the relatively slow oxygen reduction reaction kinetics, which is key in the pursuit to increase the overall efficiency of the cell.

In addition to the inherent benefits to the oxygen reduction reaction, an effective polymer exchange membrane should have high proton conductivity and immobilized anions. It should be insoluble in water but water should be soluble in the membrane. The membrane should be impermeable to hydrogen and oxygen (low crossover). There should exist dimensional stability as well as chemical and electrochemical stability during operation, thermal stability, and tolerance to impurities. In terms of the water management issues mentioned earlier, the membrane should exhibit swift water transport and reversible hydration. As with other components of the MEA, there is some conflict in

the membrane design requirements: low protonic resistance requires high ion exchange capacity and low thickness, which has to be balanced with the requirements of high physical stability and low crossover. Although adjustments can be made to the polymer exchange membrane in order to increase the overall efficiency of the fuel cell, the electrodes themselves and the catalyst layer also have room for improvement – particularly in the case of the oxygen reduction reaction at the cathode.

### C. Electrode Structure

In addition to maximizing the performance of the polymer electrolyte membrane, it is also important to take into consideration the various components of the electrode structure, mainly the gas diffusion layer and the catalyst layer. William Grove discovered in the mid-19$^{th}$ century that the chemical reactions in a fuel cell take place at the line where the liquid phase, gas phase, and solid platinum catalyst meet and that the core problem is to obtain "anything like a notable surface of action".[xxvi] The number of reaction sites at this three-phase boundary is much smaller than at a two-phase boundary. Grove therefore platinized the platinum to create a porous electrode structure of high surface area to increase the "surface of action", or the region in which the chemical reactions take place on the electrode surface. Grove also found that it was necessary to cover the catalyst agglomerates with a thin film of electrolyte. Mond and Langer improved upon these advancements in fuel cell design by using a non-conducting porous diaphragm or matrix to hold the liquid electrolyte and a powdered electrocatalyst in the form of platinum black. These early developments demonstrated the necessity of having a thin film of electrolyte over the electrode with access to the reactant gases while avoiding drying or drowning, having a high surface area for reaction, having an invariant

electrolyte, and analyzing the performance of fuel cells using current-voltage curves. Each of these concepts is incorporated in current fuel cell designs and has been implemented in the work presented in this paper.

Electrode material should facilitate the reduction of the activation overpotential at the desired output currents and also facilitate mass transfer to the reactant sites. An electrode material with a rough surface increases the current under the activation control at any overpotential per apparent square centimeter by a factor equal to the ratio of the real area of the roughened surface to its apparent area. The maximum increase in apparent current density obtainable with roughened surfaces is by a factor of about 100. However, the rates of diffusional processes are not greatly enhanced, unless the depths of roughness are at least of the order of magnitude of diffusion-layer thickness.[xxvii] The use of porous media does however increase the rates of diffusional processes, thereby facilitating mass transfer to the reactant sites and increasing the overall efficiency of the fuel cell. Porous media generally consists of a catalyst such as platinum distributed in the form of small particles in a porous substrate (commonly porous carbon). This porous material possesses a greater surface area and a smaller diffusion-layer thickness than planar electrode material, which results in an increase in current density.[xxviii] Within many pores, there is a thin film or meniscus of the electrolyte and the reactant gases can reach the electrode by diffusion of the dissolved gas through this film or meniscus. In these cases, diffusion-layer thickness is of the order of the thickness of the film, enabling high limiting currents to be obtained as compared to those obtained with planar electrodes. The gas diffusion layer, which is typically comprised of a thin layer of carbon particles on the surface of the porous carbon substrate, must be optimized so that reactant gases may easily diffuse, yet,

at the same time water, which travels in the opposite direction, must not accumulate in the pores. This diffusion layer must be both electrically and thermally conductive. The gas diffusion layer also should provide mechanical support, electrical contact, optimal distribution of reactant gases, and a pore structure suitable for the removal of liquid or vapor phase water. In the work discussed in this paper, catalyst in the form of small particles is dispersed uniformly within the pores of the inert conducting substrate. By supporting the catalyst on a porous material, the quantity of catalyst is considerably reduced as compared with sheet electrodes made entirely of catalyst or with electrodeposited materials.

It has now been established that high performance electrodes should maximize the active surface per unit mass of the electrocatalyst and per unit electrode area. Barriers to reactant transport to the catalyst should be minimized. Overall, the electrode should give invariant performance with time under actual operating conditions. It is necessary that the catalyst in the electrode structure not be buried under the support and that catalyst particles have an ionic pathway for protons that presents a low barrier to oxygen permeability, a low resistance for proton transport (high conductivity), and a low barrier to water diffusion (hydrophilic pathways for removal of product water). Additionally, the electrode structure should have hydrophobic gas passages to deliver and distribute reactants to the catalyst particles. Finally, the catalyst particles must be electronically connected to the external circuit. In order to satisfy these various requirements, inks or slurries are typically formulated and applied either to the gas diffusion layer, which acts as a substrate, or directly to the membrane itself. Applying the catalyst ink to the gas diffusion layer leads to a basic two-layer structure called the catalyst coated substrate,

whereas applying the catalyst to both sides of the membrane leads to a three-layer structure called the catalyst coated membrane. Two catalyst-coated substrates are then combined with a membrane or one catalyst coated membrane with two gas diffusion layers to form a five-layer complete MEA. It is still necessary however to further examine the catalyst layer.

## D. The Catalyst Layer

### 1. The Role of Catalysts in a PEMFC

Catalysts like platinum accelerate the electrodic reactions without being consumed in the overall reaction themselves. Since one step of the electrochemical reaction in a fuel cell occurs at the electrode-solution interface and at a given electrode-solution potential difference, the catalysis in a fuel cell (electrocatalysis) is similar to heterogeneous chemical catalysis except that one or more of the intermediate steps in the overall reaction is a charge-transfer step.[xxix] The catalyst plays a role in three main processes in electrochemical reactions: adsorption, charge transfer, and surface reactions. Adsorption and surface reactions are also common in chemical catalysis and therefore, by analogy, geometric and electronic factors are expected to be important in electrochemical catalysis. A catalyst should display weak but rapid adsorption of reactant gases.[xxx] As an example of the importance of adsorption, molecular hydrogen adsorbed at a metal surface can be split into reactive hydrogen atoms. The necessary energy for breaking the bond is given by the heat of adsorption. This is the first step in the catalysis of the hydrogen reaction in a fuel cell. The entire reaction mechanism for the oxidation of hydrogen is outlined in Figure 2[xxxi].

Global reaction:

$H_2 \rightarrow 2H^+ + 2e$

Possible sequence of steps:

$H_2$ (aq) → $H_2$ (ads) (diffusion and adsorption)

$H_2$ (ads) → 2H (ads) (dissociation)

H (ads) + $H_2O$ → $H_3O^+$ (ads)
+ e (electrooxidation of atoms)

$H_3O^+$ (ads) → $H_3O^+$ (aq) (transport of $H^+$)

**Figure 2.** Reaction mechanism for oxidation of hydrogen

The additional process in electrocatalysis – the charge transfer – makes the potential at the metal-solution interface an additional factor for electrochemical reactions.[xxxii]

In heterogeneous catalysis, the reaction rate is measured by the number of moles of reactant consumed in unit time per unit area of the catalyst. In electrocatalysis, the current density at the electrode is a measure of the reaction rate. Especially in the polymer electrolyte membrane systems, the platinum catalyst loading must still be significantly reduced before market introduction can be effected on a broad basis and by increasing the efficiency of the catalyst layer, which increases the reaction rate and the current density of the fuel cell, the necessary platinum loading can be reduced. In order to increase the efficiency it is necessary to examine the geometry of the catalyst layer. Three kinds of species participate in the fuel cell reaction at the catalyst layer: gases, electrons, and protons and the reaction takes place only on the portion of the catalyst surface where all three of these species have access. Furthermore, as Grove discovered, reactions can only take place at the three-phase boundary between the electrolyte (in the case of the polymer electrolyte membrane fuel cell, the ionomer), the solid and the void phases. The reaction rate can be increased by maximizing the surface area at the three-phase boundary as well

as by optimizing the geometric, electronic, and potentiostatic characteristics of the catalyst layer.

Because the three-phase boundary between the electrolyte, the solid, and the void phases is an infinitesimally small area there exist infinitely large current densities and the reaction zone must be enlarged in order to increase the overall reaction rate or current density. Enlarging the reaction zone can be accomplished either by "roughening" the surface of the membrane or by incorporating some ionomer in the catalyst layer. It is also possible to lower platinum loadings by supporting and dispersing platinum on carbon blacks so as to obtain a higher platinum surface area. Carbon supported platinum and platinum-alloy catalysts are also used because it is relatively easy to uniformly and highly disperse the catalyst even when the loading is more than 30%. This is extremely beneficial because higher loadings are expected in order to catalyze the PEMFC reactions. Additionally, the carbon black has sufficient electronic conductivity and chemical stability under fuel cell operating conditions and carbon-supported catalysts are more stable than non-supported catalysts concerning catalyst agglomeration under fuel cell operating conditions. If the ratio of carbon support to catalyst metal is optimized, this method results in higher catalyst utilizations, lower sintering rates, and lower costs.

Noble metals have the highest catalytic activity for the electrolytic hydrogen-evolution reaction and other transition metals have intermediate catalytic power. Tables 1 and 2 show the catalytic activity of different metals for hydrogen-evolution and oxygen-dissolution reactions at $25^0$ C.[xxxiii]

| *Metal* | *Normality of $H_2SO_4$ electrolyte* | *$i_0$ amp/cm$^2$* |
|---|---|---|
| Pt | 0.50 | 1.00E-03 |
| Rh | 0.50 | 6.00E-04 |
| Ir | 1.00 | 2.00E-04 |
| Pd | 1.00 | 1.00E-03 |
| Au | 2.00 | 4.00E-06 |
| Ni | 0.50 | 6.00E-06 |
| Nb | 1.00 | 4.00E-07 |
| W | 0.50 | 3.00E-07 |
| Cd | 0.50 | 2.00E-11 |
| Mn | 0.10 | 1.00E-11 |
| Pb | 0.50 | 5.00E-12 |
| Hg | 0.25 | 8.00E-13 |
| Ti | 2.00 | 6.00E-09 |

**Table 1.** Exchange Current Densities for the Hydrogen-electrode Reaction on Some Metals in $H_2SO_4$ at $25^0$ C.

| *Metal* | *$i_0$ in* 0.1 *N* $HClO_4$ (pH ~ 1), *amp/cm$^2$* | $i_0$ in 0.1 *N* NaOH (pH ~ 12), *amp/cm$^2$* |
|---|---|---|
| Pt | 1.00E-10 | 1.00E-10 |
| Pd | 4.00E-11 | 1.00E-11 |
| Rh | 2.00E-12 | 3.00E-13 |
| Ir | 4.00E-13 | 3.00E-14 |
| Au | 2.00E-12 | 4.00E-15 |
| Ag | | 4.00E-10 |
| Ru | | 1.00E-08 |
| Ni | | 5.00E-10 |
| Fe | | 6.00E-11 |
| Cu | | 1.00E-08 |
| Re | | 4.00E-10 |

**Table 2.** Exchange Current Densities for the Oxygen-electrode Reaction on Some Metals at $25^0$ C.

Metals are characterized by the presence of free electrons and each ion in the bulk of a metallic lattice is equally attracted to all of its nearest neighbors. The important physical properties of metals that are relevant to catalysis are: normal lattice structure, the melting and boiling points, the work function, the standard electrode potential, the metallic radius, the latent heat of sublimation, the density and specific resistance, and the magnetic susceptibility. The surface of a metal is not homogeneous, close-packed with all its surface atoms at the same distance from a plane parallel to it, at temperatures above absolute zero. At higher temperatures, a non close-packed or stepped surface is formed. Atoms at "kink sites" are in a state of higher energy than those in the straight portion of a step, which is in turn at a greater energy than those on sites in a homogeneous surface.[xxxiv] Because atoms in the region of the dislocation have a higher energy than the atoms on a plane surface, the energies of adsorption of reactants at geometrical defects are higher, which in turn accelerate reaction rates.[xxxv]

Alloys, as opposed to metals, are homogeneous substances consisting of two or more elements, generally metals. Substitutional alloys involve atoms of one element replacing those of another in a regular lattice. In an interstitial alloy, the atoms of the one of the components are so small that they occupy interstitial positions in a regular network of the other component without disturbing the order in the latter.[xxxvi] Not surprisingly, the surface and bulk compositions are not the same in alloys as they are for metals. New phases are formed on the surface of alloys, which are not the same in composition as that of the bulk. Compositions at grain boundaries and in crystallites are also not identical. These differences cause a difference in the number of active sites on the surface of an alloy compared with that which would exist were the surface and bulk concentrations the same.[xxxvii] The geometric characteristics of both metals and alloys are important because they determine how strongly a reactant may be adsorbed. Reactants must be sufficiently strongly adsorbed to reach a finite concentration on the surface but must not be too strongly adsorbed to permit a high enough rate constant for the subsequent desorption reaction. In other words, the catalytic activity of the surface depends on its lattice structure and spacing.

In addition to the geometric characteristics of catalysts, electronic factors come into play to affect the reaction rate or current density of the fuel cell. Transition metals are the more active known catalysts. These metals are known to strongly adsorb atomic hydrogen and oxygen as well as molecules and fragments of hydrocarbons and there are several theories for how this adsorption occurs. One theory is that the transition metals have partly filled *d* shells and, in the gas phase, the numbers of electrons in these shells increase from one to nine in each of the long periods of the periodic table. There is

electron overlap of the *d* levels with the immediately higher *s* level and when hydrogen enters the metal it is iononized and the free electrons enter the vacant *d* orbital. However, this theory is only valid for the group VIII metals and not for the transition metals preceding it.[xxxviii] The more generally applicable theory is the Valence-Bond Theory, which states that metals having more unpaired electrons in the *d* band have a lower percentage *d*-band character and would pair with unpaired electrons from donating atoms or molecules.[xxxix]

The work function (Φ), the energy required to remove an electron from the bulk of the metal to a point well outside it, increases with the increase in percentage of *d*-band character (more electrons are paired and a higher energy is required to extract an electron from a metal). Since the work function increases with the *d* character and the heat of adsorption of a species on the metal (ΔH) decreases with an increase in percentage of *d* character, then it follows that ΔH decreases with an increase of Φ. If adsorption is the slow step of the reaction, it can be presumed that the catalyst should have a lower percentage *d*-band character. The converse holds true if the rate-determining step is desorption.[xl] [xli] The driving force of an electrode reaction is controlled by electrical forces, which affect the charge transfer through the interface. A change in the electrode potential, which can be altered in an electrochemical cell by an external voltage, leads to a change in electronic structure (e.g. a change in electronic work function). This phenomenon, known as non-faradaic electrochemical modification of chemical activity (NEMCA), can also influence the rate of a heterogeneous chemical reaction.[xlii] Therefore, geometric and electronic factors as well as external voltages must be considered when attempting to ascertain the best catalyst for a specific reaction.

The overpotential losses in most electrochemical converters arise predominantly due to the slowness of the oxygen-reduction reaction and this is the principal problem in hydrogen-oxygen fuel cells.[xliii] If it were possible to make the reaction increasingly reversible, fuel cells could approach the ideal efficiency predicted by the Gibbs free energy and enthalpy values of the oxidation of hydrogen.[xliv] The oxygen-reduction or oxygen-dissolution reaction (hereinafter, "ODR" or "ORR") is relatively slow compared with other electrodic reactions (see Table 3).[xlv]

| *Reaction* | *Electrode Material* | *Exchange current density: - log $i_0$ ($i_0$, amp/cm$^2$)* |
|---|---|---|
| $2H^+ + 2e_0^- \rightarrow H_2$ | Pt | 3.0 |
| $Cl_2 + 2e_0^- \rightarrow 2Cl^-$ | Pt | 3.0 |
| $Ag^+ + e_0^- \rightarrow Ag$ | Ag | 1.0 |
| $Fe^{3+} + e_0^- \rightarrow Fe^{2+}$ | Pt | 2.1 |
| $Hg_2Cl_2 + 2e_0^- \rightarrow 2Hg + 2Cl^-$ | Hg | 0 |
| $O_2 + 4H^+ + 4e_0^- \rightarrow 2H_2O$ | $Ba_{0\text{-}5}TaO_3$ | 6.0 |

**Table 3.** A Comparison of Exchange Current Densities for Several Reactions with That of the Oxygen-dissolution Reaction at $25^0$C

Therefore, when the ORR carries a practical density of current, a large overpotential is typically observed along with a corresponding decrease in the energy-conversion efficiency. Even at the lowest current density, there is a loss in potential of the oxygen electrode from the reversible electrode potential by 0.2 or 0.3 volt. The maximum energy-conversion efficiency of a converter is hence decreased by some 25%.[xlvi] Depending on the catalyst, the ORR goes over a four-electron (direct) pathway or a peroxide pathway, involving $H_2O_2$ as intermediate product. In acid solutions the reactions are:

**Eq. 6.** $O_2 + 4H^+ + 4e^- \rightarrow 2H_2O$ (direct pathway)
**Eq. 7.** $O_2 + 2H^+ + 2e^- \rightarrow H_2O_2$ (peroxide pathway)

In the case of platinum and platinum-family metals, where direct four-electron reduction is found, two main proposals exist for the first reaction step: Proton transfer simultaneous with charge transfer, in which case the rate determining step should be $O_{(ads)} + H^+ + e^- \rightarrow$ products, and dissociative chemisorption of $O_2$, probably simultaneous with charge transfer. In this second case, proton transfer should play no role in the reaction rate.[xlvii]

2. Platinum and Platinum Alloy Catalysts

Platinum, which is the most common catalyst for a PEMFC, has high catalytic activity towards hydrogen oxidation with exchange current densities on the order of $10^{-3}$ $A/cm^2_{Pt}$. The anode platinum loadings in the case of pure hydrogen operation can be reduced to 0.05-0.10 $mg_{Pt}/cm^2$ without any cell voltage losses.[xlviii] Oxygen reduction at platinum is characterized under most conditions by a 4-electron reaction ($O_2 + 4H^+ + 4e^- \rightarrow 2H_2O$). Under typical conditions, the oxygen reduction intermediate species share the electrode surface with platinum oxide and/or hydroxide compounds as well as other adsorbed species. The formation of platinum oxide and/or hydroxide compounds shows an irreversible behavior and so the performance of a platinum electrode may also depend on its history. The sensitivity of the reaction to other adsorbed species means that great care must be taken to avoid some types of trace impurities.[xlix] It is important to note that impurities at either the anode or the cathode have a marked effect on the relations between over-potential and current density for reactions. They may be strongly adsorbed at the active sites and thus reduce the exchange current density of the desired reaction. Impurities may also influence the free energy of adsorption of reactants or intermediates and thereby alter the exchange current density.[l] For example, if there is any carbon

monoxide in the fuel gas it will be adsorbed on the platinum anode and inhibit the dissociation of hydrogen into protons and electrons.

Further reductions in the cathode platinum loadings are still required for large-scale fuel cell applications. Unfortunately, the oxygen reduction reaction kinetics on platinum are approximately five orders of magnitude slower than the hydrogen oxidation kinetics so that reduction in cathode platinum loadings to commercial targets without compromising performance is a significant technical challenge. As with the hydrogen-reduction reaction, platinum appears as a top catalyst for the ORR, together with some of its alloys involving some first-row transition metals. The oxygen reduction reaction has a thermodynamic redox potential ($E^0$) of 1.229 V at $25^0$ C. However, the reaction is irreversible. The exchange current density on platinum electrocatalysts is the $10^{-11} – 10^{-9}$ $A/cm^2$ in both acidic and alkaline solutions and platinum has been known to be the best electrocatalyst.

In order to compensate for the slower oxygen reduction reaction kinetics, carbon-supported platinum alloys have been used with some success as oxygen reduction catalysts in phosphoric acid fuel cells. In the 1980s, it was discovered that platinum alloys were more active and stable in corrosive environments than unsupported or supported platinum-only catalysts. While the use of carbon black support materials allow platinum to be finely dispersed, maximizing active surface area, these pure platinum catalysts were shown to deactivate with time due to a loss of active area due to platinum particle agglomeration (sintering). The carbon supported platinum alloys with a high surface area however have been shown to be more active and stable as oxygen reduction catalysts. Platinum alloys have been found to be 1.5-2 times as active as platinum in

terms of mass activity and 2-4 times as active in terms of specific activity, which is the best representation of intrinsic kinetic activity of the catalyst.[li] The predominant hypothesis for the improved catalysis involves the shortening of the Pt/Pt distance. Mukerjee *et al* conducted a systematic study of five binary alloys of Pt with the first row transition elements ranging from Cr to Ni for the catalysis of the ORR and found that all alloy electrocatalysts enhanced ORR activity. The highest active binary alloy was found to be Pt/Cr, where a three-fold enhancement was reported. The activation energy for ORR was reported to be approximately half that of Pt, but the reaction order with respect to molecular oxygen was reported to be one. The conclusion therefore was that the surface nature of these alloys was more kinetically facile towards higher ORR kinetics.[lii]

A subsequent study by Watanabe *et al* examined the effect of Pt alloys with Fe, Ni and Co, where maximum activity was reported with 30% Fe, 40% Ni, and 50% Co. The kinetic current was enhanced by an order of 10, 15, and 20 times respectively. A study by Lima *et al* examined the kinetics of the ORR in KOH electrolyte on ultra thin layer electrodes formed by Pt-V, Pt-Cr, and Pt-Co electrocatalysts dispersed on a carbon powder. There was shown to be an increase of the occupancy of the Pt 5d band and some reduction of the Pt-Pt interatomic distance in the different metal alloys compared to Pt/C. Furthermore, alloys with ordered structures exhibit improved catalytic activity compared to Pt and disordered Pt alloys and the catalytic activity increases with the extend of ordering.[liii] The highest electrocatalytic activity was shown by the Pt-V/C alloy.[liv] Yet, the reaction rate for the ORR is still too slow with these catalysts, inspiring studies to assess the role that adsorbed non-intermediate species play in inhibiting the ORR. It has been shown that strong adsorption of anions, such as phosphoric acid, halide, or hydrogen

anions, changes the role of surface structure on the ORR.[lv] Thus, efforts to improve upon the platinum cathode catalyst in PEMFCs have focused on alloys that prevent an insulating anodic film, probably consisting of adsorbed OH, from inhibiting oxygen reduction.[lvi] It appears that platinum alloy catalysts, as compared to platinum, cause both a deceleration of oxide formation and a resistance to restructuring, both of which contribute to the enhanced oxygen activity in PEMFCs.

Toda *et al* explained the increase in catalytic activity of Pt alloys based on increases in Pt 5d band vacancy, leading to a stronger Pt-$O_2^-$ interaction, which causes a weakening and lengthening of the O-O bond and its easier scission. This in turn results in an increase of the reaction rate of the oxygen-reduction reaction. Arico *et al* and Shukla *et al* have attributed the increase of the catalytic activity to a decrease of the coverage of surface oxides and an enrichment of active Pt sites. Mukerjee *et al* have explained the increase in catalytic activity due to the decrease of the Pt-Pt distance and the Pt-Pt coordination numbers. Unlike Toda *et al*, Min. *et al* have suggested that oxygen reduction activity increases with the occupancy of the Pt 5d band because there is a decrease in the adsorption strength of oxygenated species resulting in a raise of the kinetics of the reduction of reaction intermediates. It has also been observed that for Pt-based catalysts in acid media, the specific activity for the ORR generally increases with decreasing surface area, which indicates that oxygen reduction on platinum is structure-sensitive.[lvii]

It has been found that the incorporation of a polyvalent transition-metal atom such as molybdenum or vanadium into a noble metal such as platinum causes a decrease in the rate of hydrogen evolution at low overpotentials but an increase in the rate at high overpotentials, as compared with the rates in the corresponding overpotential regions on

the pure metal. Alloying with polyvalent metal atoms reduces the work function, the energy required to remove an electron from the bulk of the metal to a point well outside it, and the observed behavior may be explained on the basis of a slow-recombination mechanism in the low-overpotential region and a slow-discharge step in the high-overpotential region.[lviii]

Although carbon-supported platinum and platinum alloys have been shown to be effective catalysts in a PEMFC, platinum easily adsorbs the oxygen at the cathode, making it difficult for the protons to adsorb. It has been hypothesized that using a gold catalyst at the cathode could mitigate this problem and thereby facilitate the chemical reaction involving the recombination of oxygen with protons and electrons in order to form water. However, gold is known to be a poor catalyst. The work presented in this paper therefore focuses on the implementation of various combinations of gold and platinum catalyst materials at the cathode in order to facilitate the oxygen reduction reaction kinetics, improve the performance of the MEA, and mitigate production costs.

3. Gold and Gold Alloy Catalysts

Gold and palladium alloys have been investigated as alternatives to a solid platinum catalyst with dissatisfying results. When log $i_0$ (where $i_0$ is the exchange-current density) was plotted against percent gold composition in the alloy, there was found to be a rapid decrease of $i_0$ with increase of gold composition until a composition of 60% gold was reached. Thereafter, the decrease in $i_0$ with increase in percent of gold composition was much slower. This has been explained by the gradual filling up of the *d* band of the alloy and consequent decrease in the rate of hydrogen evolution with increase in gold composition from 0 to 60% gold. At 60% gold composition, the *d* band is completed in

the alloy and thus between 60 and 100% gold in the alloy, there is hardly any change in the rate of hydrogen evolution in it.[lix] The uptake of oxygen by an oxide-free metal follows dissociative adsorption – as the number of unpaired *d* electrons increases, the oxygen coverage increases. Gold, with no unpaired *d* electrons, shows the lowest coverage, whereas ruthenium and platinum, with the highest number of unpaired electrons have the highest coverage. In the case of catalysis of the hydrogen oxide reduction on Au(100) and Au(111) by lead adatoms, the presence of lead adatoms introduce important changes in the catalytic activity. The most important catalytic effect arose from unit cells where the reactant came into close contact with both gold and lead atoms, which is consistent with a dissociative adsorption mechanism due to a bimetal bridge adsorption model.[lx]

In studies of the oxygen-dissolution reaction on gold and palladium or platinum as well as their alloys, it was found that their Tafel slopes changed sharply at a composition greater than 50% gold. It is probable that this change actually occurs at 60% gold, 40% palladium or platinum, at which composition the *d* band is completed when adding increased amounts of gold to palladium or platinum.[lxi] Enhanced activity was observed with the use of gold single crystal surfaces when covered by thin palladium layers. Gold, having no unpaired d-electrons, is unique among the metals studied for oxygen reduction because of its lack of ability to adsorb oxygen and its high potential for oxide formation. Reactions are complex and include oxygen reduction, peroxide reduction, peroxide oxidation, and peroxide decomposition with intermediates diffusing between sites of different activities. In contrast to platinum, gold's activity can be greatly enhanced by some impurities (most notably in the case of metal underpotential deposition).[lxii][lxiii] This

has been most notably reported for platinum ions corroded from other electrodes in the electrochemical cell, which is pertinent to the work described in this paper because of the suggestion of synergies between platinum and gold as an effective combinatorial catalyst. Oxygen reduction on gold is first order in $O_2$, pH independent, and has a Tafel slope of approximately –120 mV decade$^{-1}$. In alkaline electrolyte the oxygen reduction reaction occurs via direct 4e$^-$ oxidation at potentials near 0.9 V. In acid electrolyte, the ORR polarization curves on Au surfaces are shifted negatively by hundreds of mV and the reaction becomes structure insensitive.[lxiv] Therefore the rate determining step is thought to be: $S + O_2 + e^- \rightarrow S - O_2^-$. However, in some cases, the initial adsorption has been thought to be the rate-determining step. If platinum and gold were used as a combinatorial catalyst on the cathode, it could be possible to reap the benefits of platinum's high adsorption activity and catalytic activity as well as gold's lack of adsorption activity.

## III. LABORATORY PROCEDURE

The MEAs for this experimental work were assembled in the Bocarsly Fuel Cell Laboratory at Princeton University. Carbon cloth (no catalyst, carbon only) was used as the electrode material and gas diffusion layer. The carbon cloth has been purchased with the gas diffusion layer already in place. This gas diffusion layer, which is comprised of carbon particles, is designed so as allow for the diffusion of reactant gases and the transport of product water and is both electrically and thermally conductive. The electrode material and gas diffusion layer provide mechanical support, electrical contact, optimal distribution of reactant gases, and a pore structure suitable for the removal of liquid or vapor phase water. Catalyst slurries were created by sonicating a total of 0.050 g ETEK 20% platinum on Vulcan carbon (by weight) and ETEK 20% gold on Vulcan carbon (by weight) with approximately 10 g isopropanol for more than thirty minutes for a metal concentration of approximately 4 mg/ml. Each slurry was created with a specific weight ratio of platinum to gold in order to determine the appropriate ratio for optimizing overall MEA performance. Each slurry was named according to the percent of the catalyst material comprised of 20% gold on carbon. For example, the slurry containing 75% gold and 25% platinum was named "75". For slurries that contained only gold or only platinum catalyst the names were "Au" and "Pt" respectively. The approximate catalyst weights used in each slurry are presented in Table 4 below.

| Slurry | Pt | 25 | 40 | 50 | 60 | 75 | Au |
|---|---|---|---|---|---|---|---|
| Weight of Pt (g) | 0.050 | 0.0375 | 0.030 | 0.025 | 0.020 | 0.0125 | 0.000 |
| Weight of Au (g) | 0.000 | 0.0125 | 0.020 | 0.025 | 0.030 | 0.0375 | 0.050 |

**Table 4.** Catalyst slurry compositions

Each of these slurries were sonicated and airbrushed on a piece of carbon cloth measuring approximately 1 inch by 2 inches (12.9 $cm^2$), using compressed nitrogen as the airbrushing gas, giving a catalyst loading of approximately 12.7 ml/12.9 $cm^2$ or 3.9 mg of catalyst per square centimeter.

**Figure 3.** Airbrush used for spraying technique

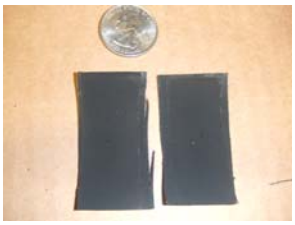

**Figure 4.** Carbon cloth electrode material after being sprayed

Once the carbon-supported catalyst and isopropanol solution on the carbon cloth electrode has dried in an 80º C oven, a solution of 5% Nafion (approximately 0.25 g) and isopropanol (approximately 5 g) that has been lightly swirled is sprayed over top of the platinum catalyst. The Nafion concentration is 5% of 250mg/3.9 ml, or 3.2 mg/ml. This gives a Nafion loading of approximately 0.09 mg/$cm^2$. Carbon-supported catalyst is used for several reasons. Mainly, the carbon black support makes it possible to easily disperse the catalyst uniformly, increasing the platinum surface area, even at loadings higher than 30%. Furthermore, the carbon black is electronically conductive and chemically stable under fuel cell operating conditions causing carbon supported catalysts to be more stable than non-supported catalysts concerning catalyst agglomeration under fuel cell operating conditions. The Nafion layer serves several purposes: it facilitates adhesion between the different components of the MEA and also encourages water removal at the membrane-electrode interface. Furthermore, as discovered by Grove, incorporating some electrolyte

material in the catalyst layer increases the reaction zone at the three-phase interface on the surface of the electrode.

Once the rectangular electrode has been created it is trimmed into two 0.875 inch by 0.875 inch squares to produce two electrodes. For each MEA, two electrodes are placed in between two pieces of rubber gasket material within the diamond-shaped holes cut for this purpose. A Nafion 115 membrane that has been prepared and stored in distilled water is placed in between the two electrodes making sure that the catalyst side of each electrode is facing the membrane. The entire assembly (see Figure 5) is then placed in a hot press, the force of the press is set at 1 ton (with pressure equal to 1 ton/4.93 $cm^2$) and the temperature variacs are switched on. When the temperature has reached approximately 140º C, the variacs are switched off and the temperature is allowed to float up to as much as 150º C. The force is then raised to 2 ton for a period of 60 seconds after which the MEA is placed underneath a weight to cool and then stored in a humid environment until testing. Originally the pressing technique did not call for any pressure in the heating stage (variacs were switched off at 135º C), and then a force equal to 1 ton after allowing the temperature to float up to 145º C. Due to the poor adhesive quality of the first few electrodes the technique was adjusted as necessary with favorable results.

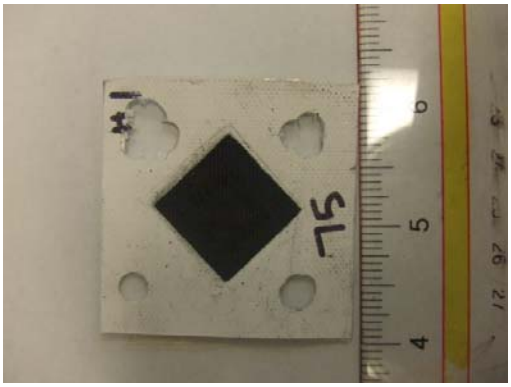

**Figure 5.** Finished MEA

Each MEA is tested at two temperatures (60 and 90 $^0$C) and two relative humidities (hydrogen and oxygen flow rates of 12.0 ml/min and 6.0 ml/min respectively

and 8.0 ml/min and 4.0 ml/min respectively) for a total of four, two-hour tests per MEA. The laboratory setup with flow and temperature controllers, fuel cell hardware, and connections to computer is shown in Figure 6.

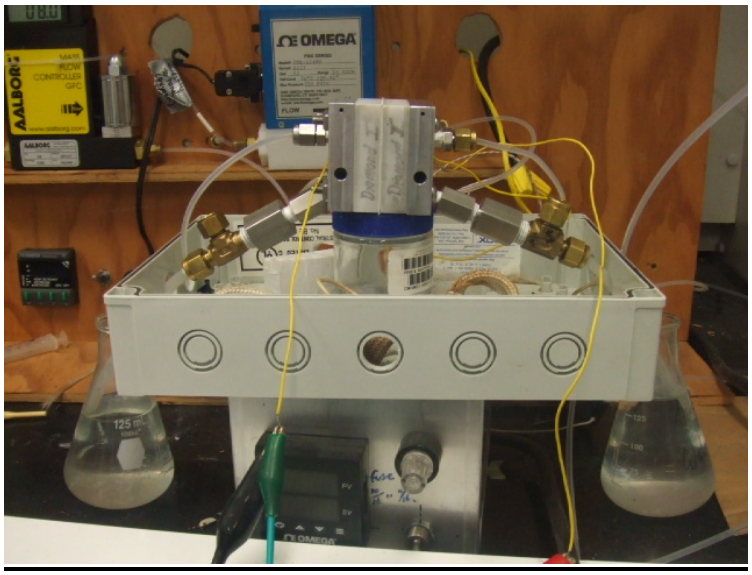


**Figure 6.** Laboratory setup for testing of MEAs

The data is collected using the Arbin testing software and hardware in Jay Benziger's laboratory. The fuel cell was started for each test by using a rest step, then resetting all variables. The current was then allowed to equilibrate at 0.5 amps for one hour. Each test consisted of three CV sweeps, with sweep rate equal to 1 second, resetting the current to 0.5 amps before and after each sweep and allowing the current to re-equilibrate for 30 minutes prior to a CV sweep. CV refers to a method of electrochemical analysis called cyclic voltammetry. "Conventionally, CV involves a bi-directional linear voltage ramp applied between the electrodes of a sample in order to identify and characterize certain electrochemical processes."[lxv] ***MITS Pro*** is able to perform this test through the use of Voltage Ramp steps (one forward step, one reverse). For each test, a graph was outputted in Excel displaying the three current-voltage sweeps or polarization curves. The fuel cell

performance is characterized by its polarization curve. Three distinct regions of a fuel cell polarization curve are noticeable[lxvi]: an initial voltage drop across the membrane-electrode interface representing the activation barrier, a relatively linear middle section that represents the ohmic resistance for protons to cross the membrane, and a voltage drop in the high current regime due to mass transfer limitations.

By fitting the experimental results to one of the equations describing the polarization curve, information may be gained about the parameters of the polarization curve such as reversible cell potential, $V_r$; apparent exchange current density, $i_o$; Tafel slope, b; cell resistance, $R_i$; or limiting current $i_L$. The utility of a fuel cell is determined by its efficiency at reasonable power outputs and by its maximum power, both of which depend on the cell potential-current relation for the fuel cell. Therefore, exchange current densities of the partial reactions play a leading role in determining the performance of a fuel cell. The initial drop in the cell potential-current relation is determined mainly by the exchange current density – the lower the exchange current density, the greater is this drop, and hence the greater the loss of efficiency and power.[lxvii] In order to perform quick calculations regarding fuel cell efficiency, a linear approximation of the ohmic resistance portion of the fuel cell polarization curve can be easily manipulated (avoiding the use of data in the activation and mass transfer regions). Figure 7 demonstrates this method.

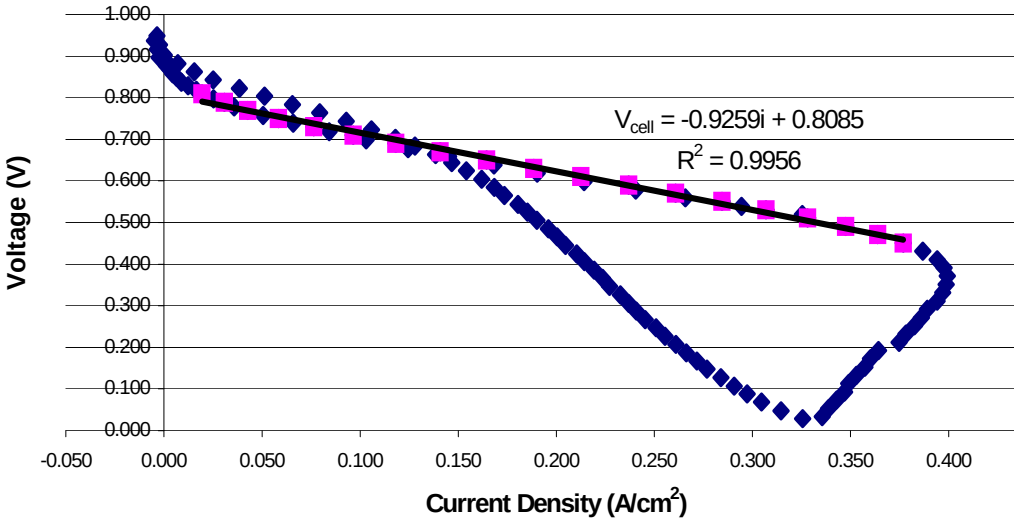


**Figure 7.** Platinum-Platinum MEA #2, $60^0$ C, 8.0 $H_2$, 4.0 $O_2$

The linear polarization curve has the following form (Eq. 8):

$$V_{cell} = V_0 - k * i$$

**Eq. 8.** Linear polarization curve

where $V_0$ is the intercept (the actual open circuit voltage is always higher), k is the slope of the curve, and i is the current density.[lxviii]

The power density as a function of cell potential can be calculated using Eq. 9.[lxix]

$$w = \frac{V_{cell}(V_0 - V_{cell})}{k}$$

**Eq. 9** Power density

It can be shown that the maximum power density is equivalent to the intercept squared divided by four times the slope (see Eq. 10).[lxx]

$$w_{\max} = \frac{V_o^{\,2}}{4k}$$

**Eq. 10** Maximum power density

This maximum power density is reached at a cell potential equivalent to half the intercept (see. Eq. 11).[lxxi]

$$V_{cell}\,|_{w\max} = \frac{V_o}{2}$$

**Eq. 11** Cell potential at which maximum power density is achieved

## IV. RESULTS AND DISCUSSION

Using the equations explained above, the maximum power densities were calculated for each of the MEAs at each of the testing conditions. The power density represents how much power can be obtained per square centimeter of electrode material and is thus a fair representation of the amount of power generated per catalyst loading. The names of the MEAs in the table below refer to the composition of the catalyst layer at the cathode. Please see the bibliography for the location of all data files. Maximum power densities for the low temperature, high relative humidity testing condition are shown in Table 5.

| MEA | k | $V_0$ | $w_{max}$ (W/cm$^2$) |
|---|---|---|---|
| Pt #1 | 1.71 | 0.806 | 0.0953 |
| Pt #2 | 0.995 | 0.784 | 0.155 |
| | | **AVG** | **0.125** |
| | | | |
| 25 #1 | 0.926 | 0.809 | 0.176 |
| 25 #2 | 1.03 | 0.777 | 0.146 |
| | | **AVG** | **0.161** |
| | | | |
| 40 #1 | 0.964 | 0.775 | 0.156 |
| 40 #2 | 0.715 | 0.779 | 0.212 |
| | | **AVG** | **0.184** |
| | | | |
| 50 #1 | 0.818 | 0.763 | 0.178 |
| 50 #2 | 1.10 | 0.810 | 0.149 |
| 50 #3 | 0.987 | 0.743 | 0.140 |
| | | **AVG** | **0.159** |
| | | | |
| 60 #1 | 0.766 | 0.743 | 0.180 |
| 60 #2 | 0.779 | 0.755 | 0.183 |
| | | **AVG** | **0.182** |
| | | | |
| 75 #1 | 1.078 | 0.691 | 0.111 |
| 75 #2 | 1.108 | 0.694 | 0.109 |
| | | **AVG** | **0.110** |
| | | | |
| Au #1 | 2.61 | 0.373 | 0.0133 |
| Au #2 | 2.05 | 0.350 | 0.0149 |
| | | **AVG** | **0.0141** |

**Table 5.** Maximum power densities at $60^0$ C, 8.0 ml/min $H_2$, 4.0 ml/min $O_2$

From these preliminary calculations, it seems that a platinum-gold combination of between 40 wt. % and 60 wt. % gold on the cathode results in the highest power density. The power density seems to decrease at the 50 wt. % gold composition, peak again at the 60 wt. % gold composition, and then decrease at compositions greater than 60 wt. % gold, however, this slight decrease at the 50 wt. % gold composition is most likely not evident of a trend.

It is interesting to note the peak in power density at the 60 wt. % gold catalyst composition since studies have shown that it is also at a 60 wt. % gold, 40 wt. % palladium alloy composition that a change in current density trend occurs. As noted in the background section, there was found to be a rapid decrease of $i_0$ with increase of gold composition until a composition of 60% gold was reached. Thereafter, the decrease in $i_0$ with increase in percent of gold composition was much slower. This has been explained by the gradual filling up of the *d* band of the alloy and consequent decrease in the rate of hydrogen evolution with increase in gold composition from 0 to 60% gold. At 60% gold composition, the *d* band is completed in the alloy and thus between 60 and 100% gold in the alloy, there is hardly any change in the rate of hydrogen evolution in it. Yet, in the work presented in this paper, the gold-platinum composition is being tested on the cathode for the oxygen reduction reaction, not for the hydrogen-evolution reaction. Also, alloys are not being utilized but instead slurries of the two metals deposited on carbon particles and sonicated in ethyl alcohol. The alloy has different surface characteristics than the slurry and therefore the power density peaks at 40% and 60% wt. gold slurries cannot necessarily be explained by the completion of the d-band or the surface characteristics of the catalyst.

The results from the platinum-50 MEA #2 were particularly poor at each of the four testing conditions, with high levels of crossover occurring, as can be seen by the negative currents obtained on the IV curves (see Figure 8).

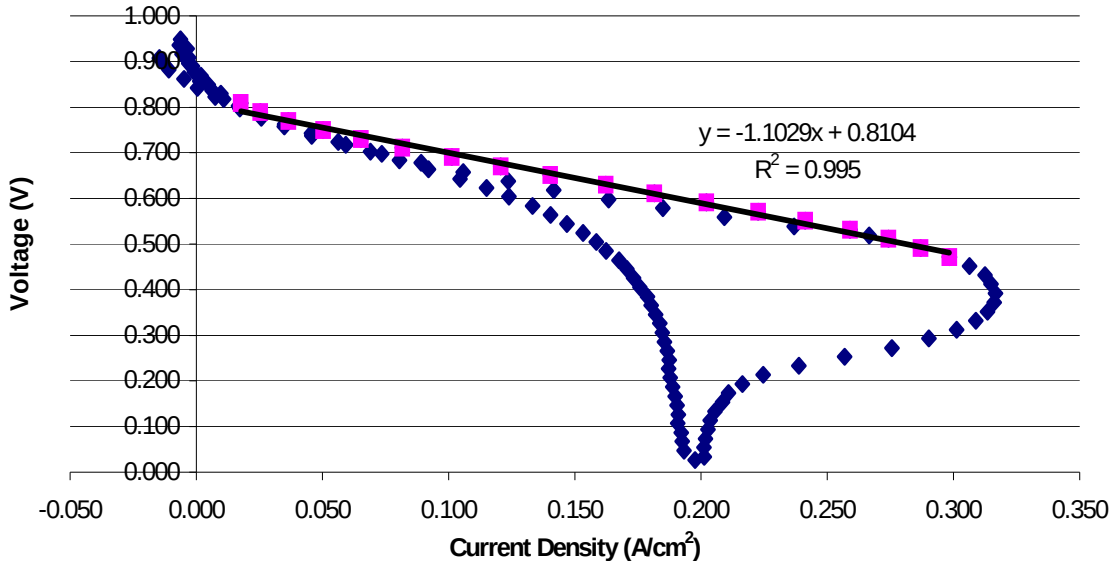


**Figure 8.** Platinum-50 MEA #2 at $60^0$ C, 8.0 ml/min $H_2$, 4.0 ml/min $O_2$

However, if the power density value for this MEA were discarded, the average power density obtained with the 50 wt. % slurries would still be 0.159 W/cm$^2$. Crossover occurs when unreacted hydrogen travels over to the cathode and results in a lower potential. This phenomenon is better explained by a deficiency in the membrane that caused hydrogen to pass through the MEA rather than a deficiency in the catalyst material itself. Regardless, the overall trend remains the same despite the poor performance of Platinum-50 MEA #2.

In Figure 8, the sharp dip in the bottom portion of the curve at approximately 0.200 A can be explained by the adsorption of the reactant gases and the consumption of those gases. A mass balance on hydrogen shows that moles of $H_2$ subtracted from moles of $H_2$ in gives the steady state current. For 100% hydrogen utilization, the steady state current is equivalent to the limiting current. The limiting current is therefore equal to:

$$\frac{(1bar)*(8cm^3/\min)*(96{,}500coulombs/mol)}{(160s/\min)*(82cm^3-bar/mol\ \ K)*(298K)}=1.05A$$

The fact that currents exceeding 1.05 A are achieved is due to the inventory of hydrogen in the flow channels and adsorbed on the electrodes that can be used up in the reaction. At 0.200 A, stored hydrogen formerly adsorbed at the anode or in the flow channels is fully consumed, causing a sharp drop in potential at 0.200 A. As more reactant gases are fed into the fuel cell and consumed by the reaction, the potential slowly increases again with decreasing current. This phenomenon occurs with several of the other MEAs at the low temperature, high relative humidity testing condition as well, most notably: Platinum-25 MEA #1 and #2, Platinum-40 MEA #2, Platinum-50 MEA #1 and #2, Platinum-60 MEA #2, and Platinum-75 MEA #2. See Figures 9 –14.

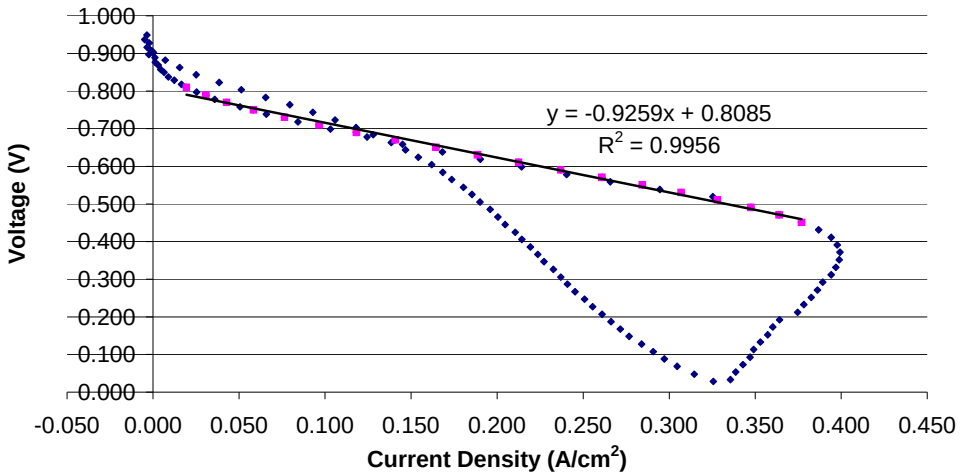


**Figure 9.** Platinum-25 MEA 1 at $60^0$ C, 8.0 ml/min $H_2$, 4.0 ml/min $O_2$

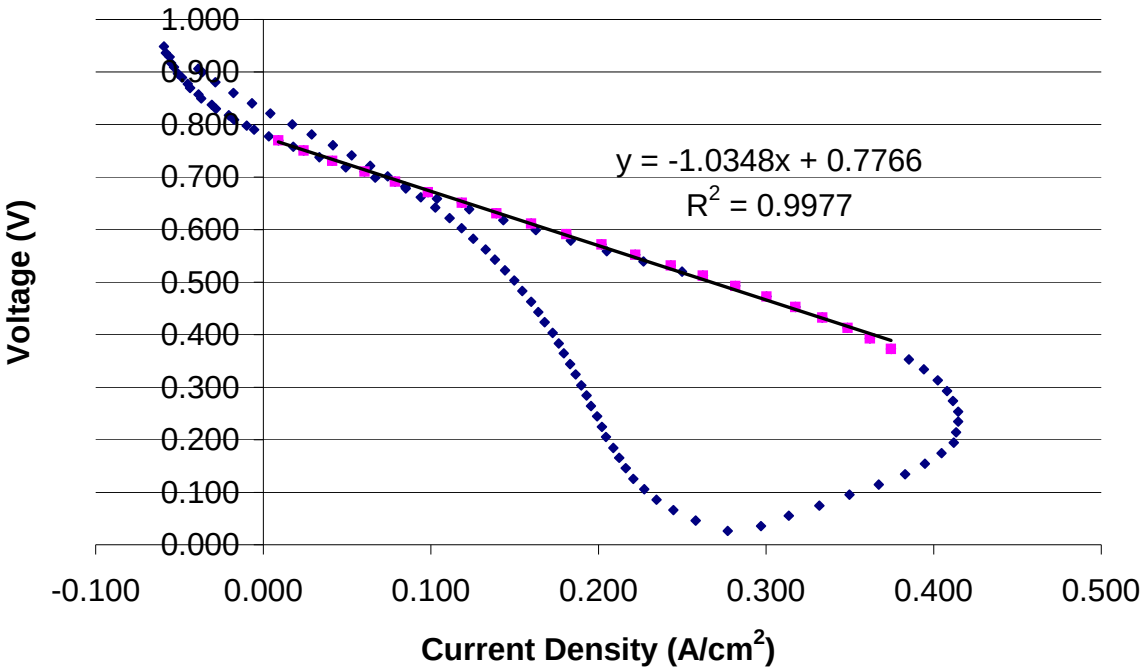


**Figure 10.** Platinum-25 MEA 2 at $60^0$ C, 8.0 ml/min $H_2$, 4.0 ml/min $O_2$

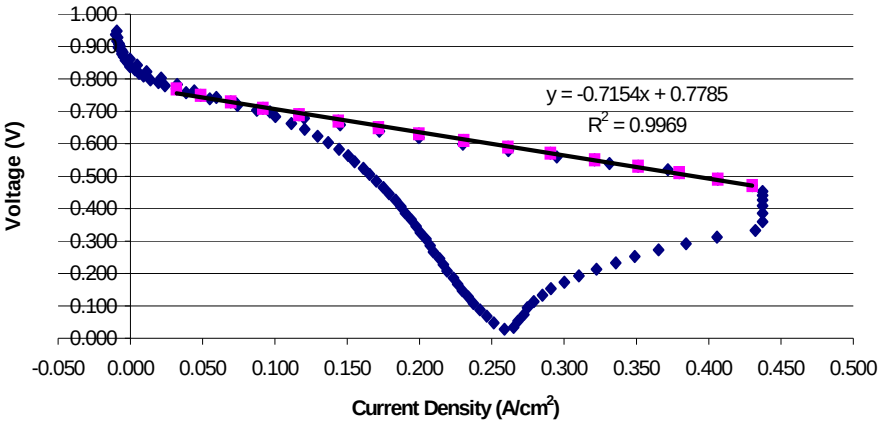


**Figure 11.** Platinum-40 MEA 2 at $60^0$ C, 8.0 ml/min $H_2$, 4.0 ml/min $O_2$

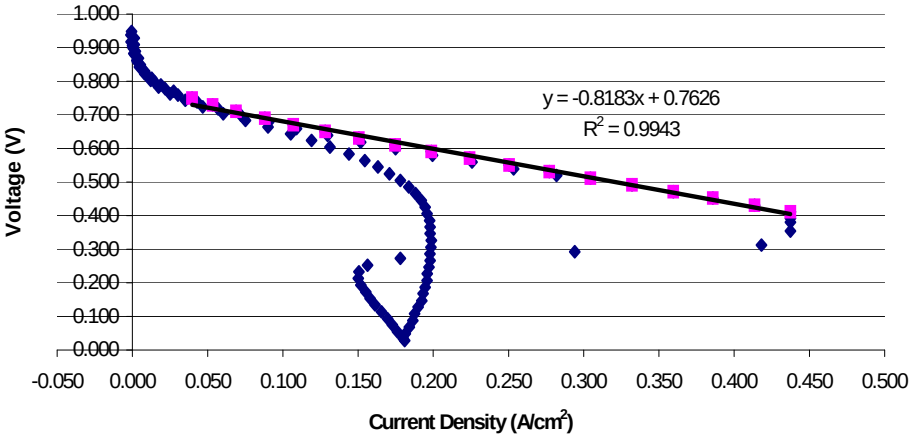


**Figure 12.** Platinum-50 MEA 1 at $60^0$ C, 8.0 ml/min $H_2$, 4.0 ml/min $O_2$

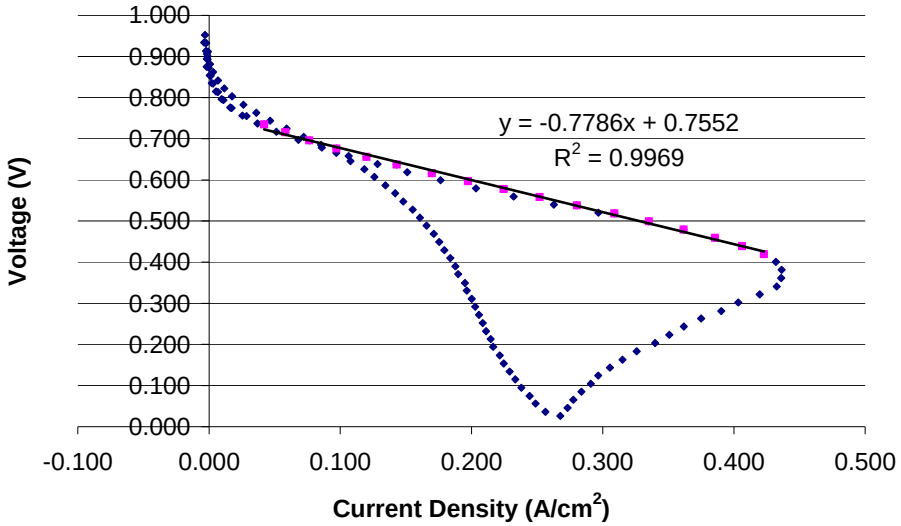


**Figure 13.** Platinum-60 MEA 2 at $60^0$ C, 8.0 ml/min $H_2$, 4.0 ml/min $O_2$

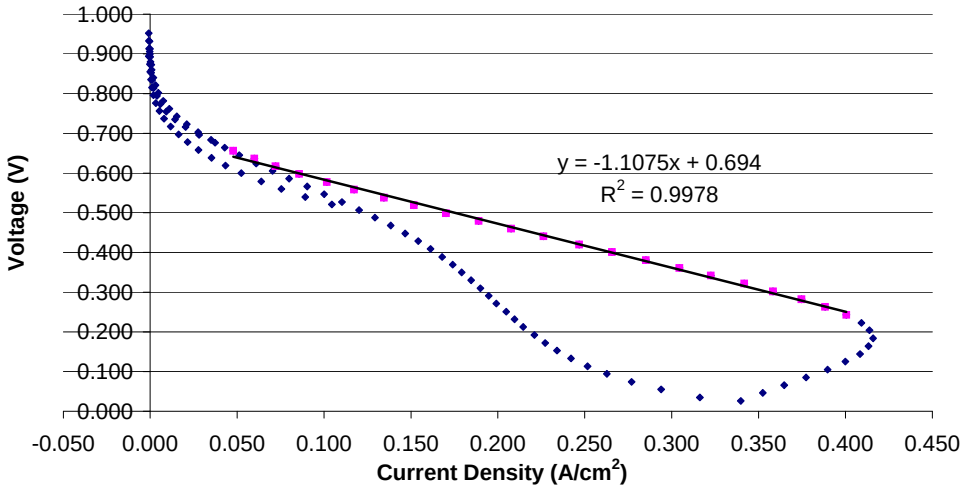


**Figure 14.** Platinum-75 MEA 2 at $60^0$ C, 8.0 ml/min $H_2$, 4.0 ml/min $O_2$

Each of these MEAs seems to have reached maximum reactant gas consumption at the electrodes at different current densities, which makes sense in light of their overall differences in performance. Because each MEA has a different combination of catalyst they have varying abilities to adsorb the reactants. As the amount of gold in the catalyst layer increases, the current density at which the adsorbed reactant gases are full consumed decreases until the 60 wt. % gold, 40 wt. % platinum catalyst combination is reached. At the 60 wt. % gold, 40 wt. % platinum catalyst combination, the current

density at which the gases are full consumed increases again. Current and voltage are both displayed verses time for the current-voltage sweep for platinum-40 MEA #2 at the first testing condition in Figure 15 so as to emphasize the linear progression of fluctuations in voltage and current as well as to explicate the mechanisms of adsorption and consumption of reactant gases.

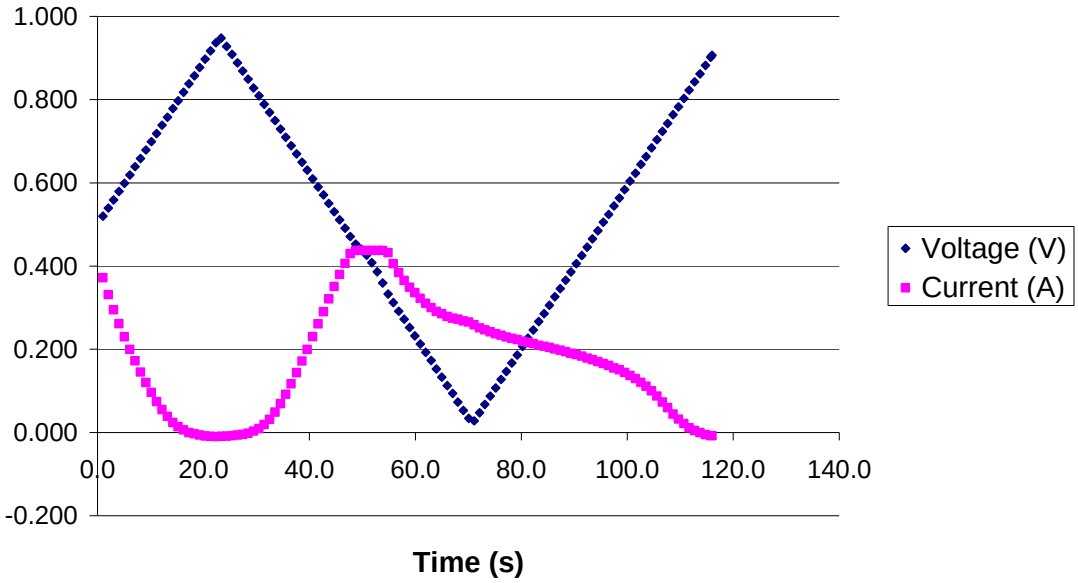


**Figure 15.** Current and Voltage vs. Time for Platinum-40 MEA #2 at $60^0$ C, 8.0 ml/min $H_2$, 4.0 ml/min $O_2$

It can be seen in Figure 15 that at a current of over 0.400 at time 58 seconds, where the voltage should bottom out, it actually is sustained until about 70 seconds. This is due to the fact that the reaction is being powered by adsorbed hydrogen and hydrogen in the flow channels for several seconds. This confirms the hypothesis that the level of surface adsorption of reactant gases and their subsequent consumption play a role in the overall performance of the catalyst layer.

At the low temperature, high relative humidity testing condition, the mass transfer limitation region of the graph was restricted due to the limitations of the Arbin instrument. The maximum current the Arbin unit will allow is 2.2 A. This is discernible

on the IV curve by a sharp drop off at 0.437 A/cm$^2$ instead of an obvious mass transfer region. See Figures 16 – 22.

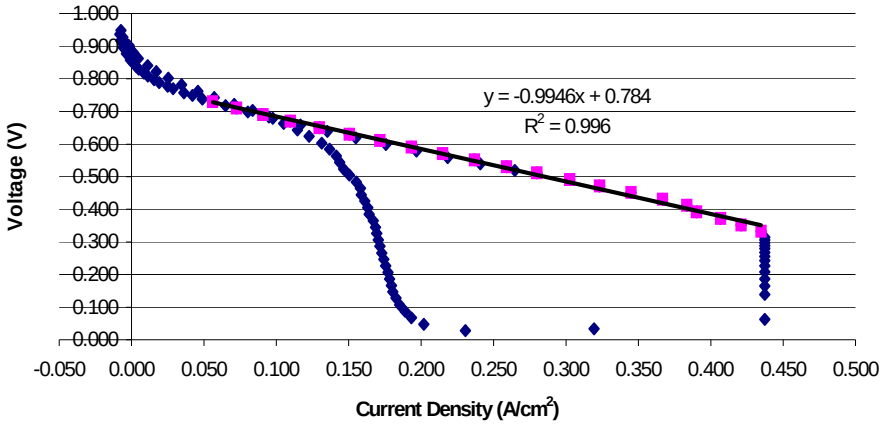


**Figure 16.** Platinum-Platinum MEA 2 at 60$^0$ C, 8.0 ml/min $H_2$, 4.0 ml/min $O_2$

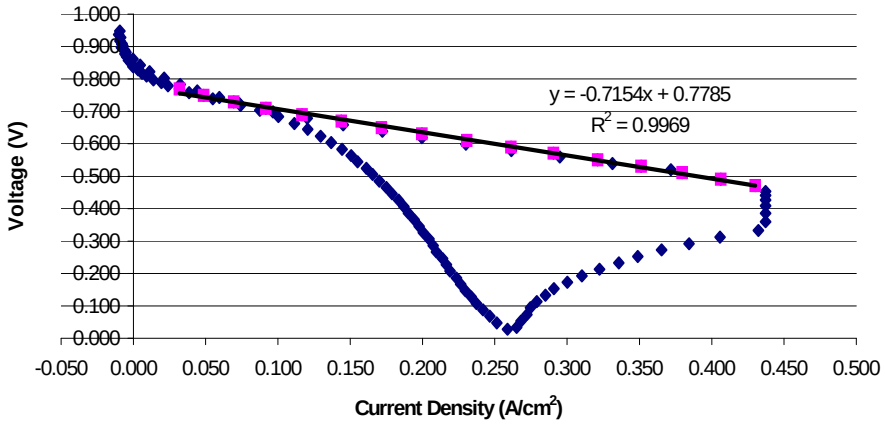


**Figure 17.** Platinum-40 MEA 1 at 60$^0$ C, 8.0 ml/min $H_2$, 4.0 ml/min $O_2$

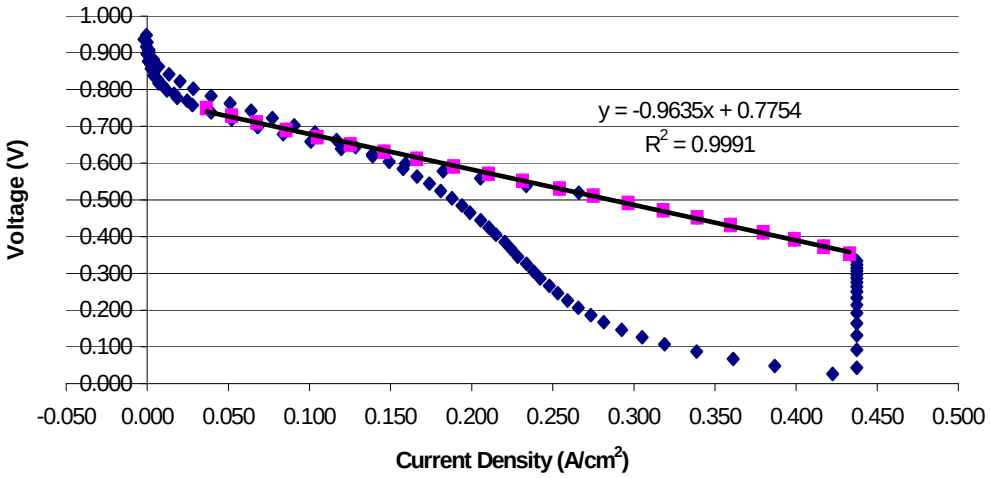


**Figure 18.** Platinum-40 MEA 2 at $60^0$ C, 8.0 ml/min $H_2$, 4.0 ml/min $O_2$

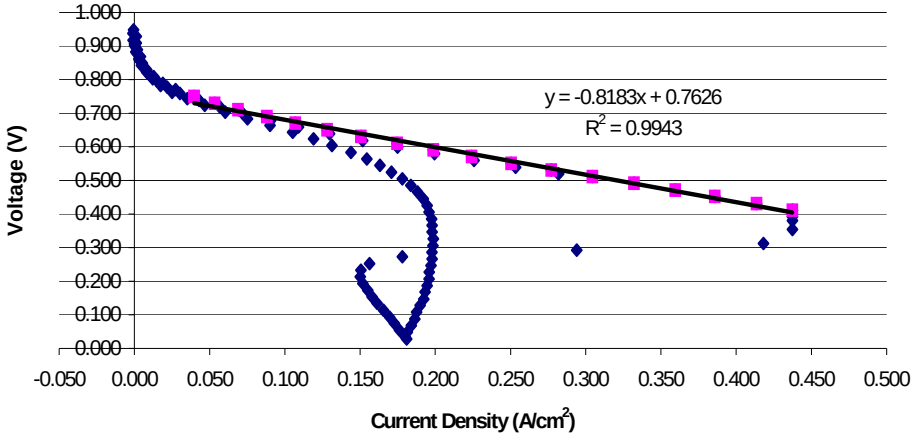


**Figure 19.** Platinum-50 MEA 1 at $60^0$ C, 8.0 ml/min $H_2$, 4.0 ml/min $O_2$

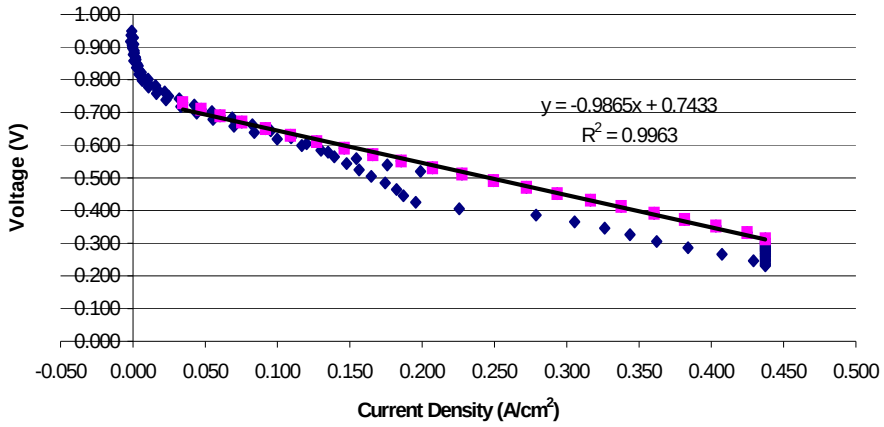


**Figure 20.** Platinum-50 MEA 3 at $60^0$ C, 8.0 ml/min $H_2$, 4.0 ml/min $O_2$

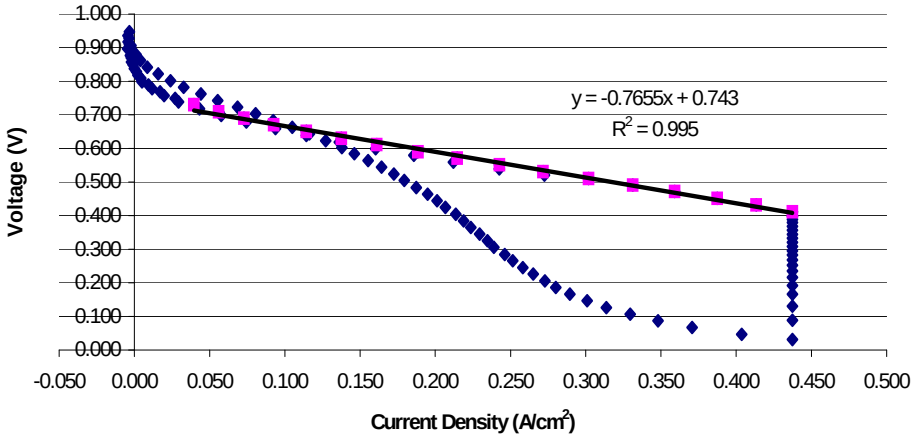


**Figure 21.** Platinum-60 MEA 1 at $60^0$ C, 8.0 ml/min $H_2$, 4.0 ml/min $O_2$

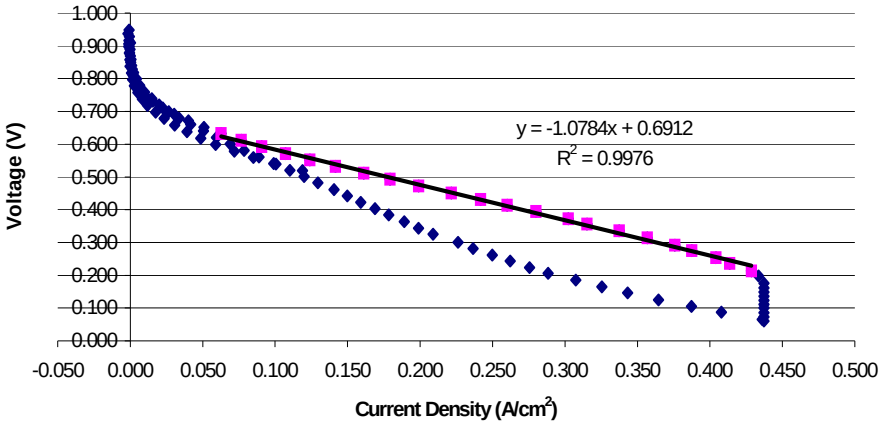


**Figure 22.** Platinum-75 MEA 1 at $60^0$ C, 8.0 ml/min $H_2$, 4.0 ml/min $O_2$

A different theory stating that this sharp drop off in potential at 0.437 A/cm$^2$ was caused by limitations induced by a lack of reactant gases was tested for Platinum-75 MEA #1 by increasing the amounts of both oxygen and hydrogen while leaving the other reactant gas at the same value as in the low temperature, high relative humidity testing conditions. The results are shown in Figures 23 – 24.

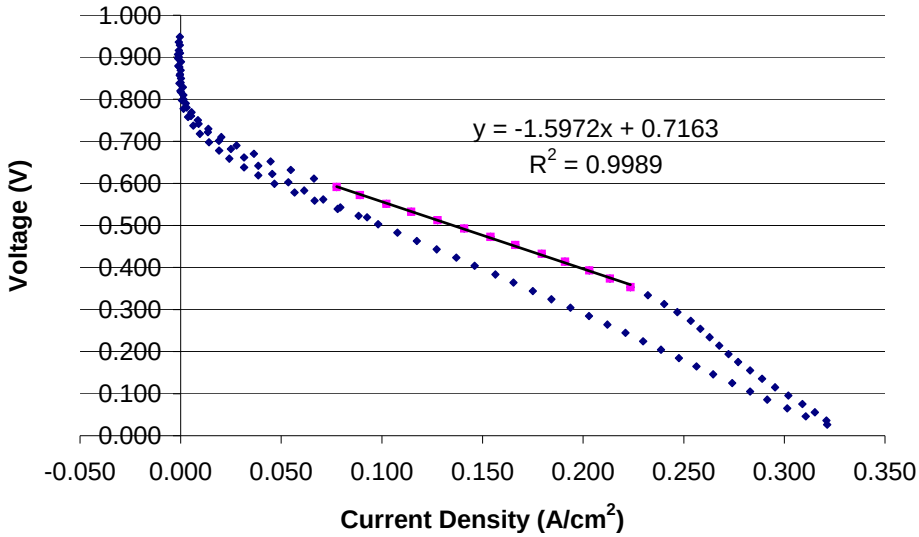


**Figure 23.** Platinum-75 MEA 1 at $60^0$ C, 8.0 ml/min $H_2$, 6.0 ml/min $O_2$

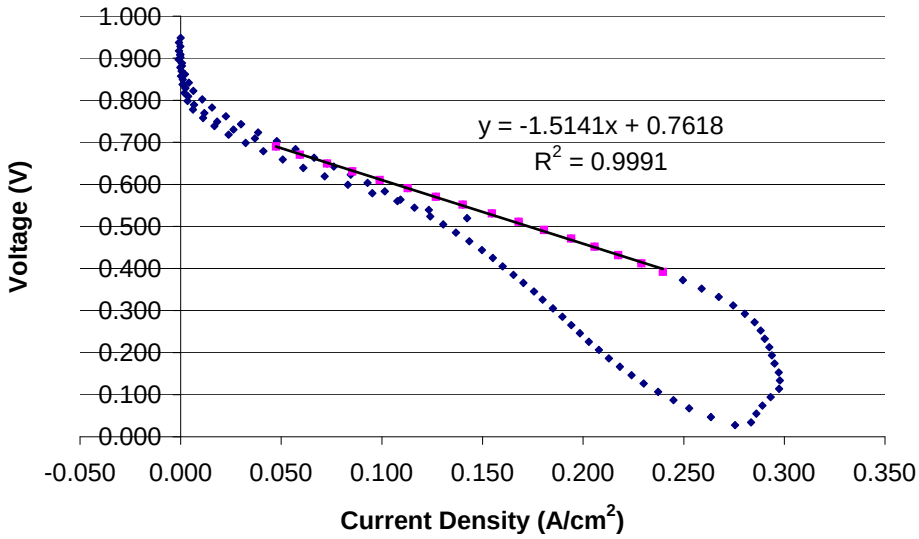


**Figure 24.** Platinum-75 MEA 1 at $60^0$ C, 10.0 ml/min $H_2$, 4.0 ml/min $O_2$

From these tests it is not clear if hydrogen or oxygen was the limiting reactant gas. In fact, they both seem to have been limiting in the case of the $60^0$ C, 8.0 ml/min $H_2$, and 4.0 ml/min $O_2$ testing condition. However, much lower current densities were achieved with the increase in hydrogen than with the increase in oxygen and both increases resulted in lower current densities than the initial condition. The lower current densities obtained

with these increases in reactant gases as compared to the initial testing condition can be explained by deterioration in the MEA in between the tests or drying out of the MEA due to higher flow rates of reactant gases. The increase in hydrogen and oxygen was tested approximately two weeks after the original testing condition. The fact that lower current densities were achieved with the increase in hydrogen than with the increase in oxygen suggests that the oxygen becomes adsorbed more easily at the surface of the catalyst, resulting in an oxygen deficiency that can be slightly remedied by an increase in oxygen flow rate. However, the reason for restriction in the mass flow limitation regime is due to instrument limitations, and not to actual mass flow limitations.

At the low temperature, low relative humidity testing condition the highest power density was achieved at the 60 wt. % gold, 40 wt. % platinum composite catalyst although there is also an extended peak in power density between the 40 wt. % gold and 60 wt. % gold compositions. The power density slowly increases with the percentage of gold until the 50% composition, at which point there is a decrease in performance, even when the power density value for Platinum-50 MEA #2 is discarded. However, it is believed that the slight decrease at 50% composition is not indicative of an actual decreasing trend at this composition. After the second peak in performance at the 60 wt. % gold composition, there is a definite decrease in performance with increasing amounts of gold. See Table 6 below.

| **MEA** | **k** | **$V_0$** | **$w_{max}$ ($W/cm^2$)** |
|---|---|---|---|
| Pt #1 | 1.88 | 0.776 | 0.0803 |
| Pt #2 | 0.992 | 0.806 | 0.164 |
| | | **AVG** | **0.122** |
| | | | |
| 25 #1 | 0.980 | 0.820 | 0.172 |
| 25 #2 | 1.42 | 0.801 | 0.113 |
| | | **AVG** | **0.142** |
| | | | |

| | | | |
|---|---|---|---|
| 40 #1 | 0.997 | 0.806 | 0.163 |
| 40 #2 | 0.792 | 0.823 | 0.214 |
| | | **AVG** | **0.188** |
| | | | |
| 50 #1 | 0.757 | 0.777 | 0.199 |
| 50 #2 | 1.07 | 0.806 | 0.153 |
| 50 #3 | 0.955 | 0.762 | 0.152 |
| | | **AVG** | **0.168** |
| | | | |
| 60 #1 | 0.748 | 0.791 | 0.209 |
| 60 #2 | 0.804 | 0.790 | 0.194 |
| | | **AVG** | **0.202** |
| | | | |
| 75 #1 | 0.924 | 0.722 | 0.141 |
| 75 #2 | 0.987 | 0.712 | 0.128 |
| | | **AVG** | **0.135** |
| | | | |
| Au #1 | 12.5 | 0.324 | 0.00209 |
| Au #2 | 2.13 | 0.421 | 0.0208 |
| | | **AVG** | **0.0115** |

**Table 6.** Maximum power densities at $60^0$ C, 12.0 ml/min $H_2$, 6.0 ml/min $O_2$

Compared to the power densities of each MEA at the low temperature, high relative humidity testing, the power densities of the MEAs at the low temperature, low relative humidity testing were lower for the platinum-platinum, platinum-25, and platinum-gold MEAs but higher for the platinum-40, platinum-50, platinum-60, and platinum-75 MEAs. The poorer performance for the platinum-platinum, platinum-25, and platinum-gold MEAs can be accounted for by drying out of the polymer membrane at the higher flow rates of reactant gases. The higher performance for the platinum-40, platinum-50, platinum-60, and platinum-75 MEAs despite possible drying out of the membrane could be accounted for by the enhanced catalytic activity of the combinatorial catalysts at higher temperatures.

Several of the MEAs also showed strong adsorption at the catalyst layer at the low temperature, low relative humidity testing condition. This is discernible by the sharp dip

in potential in the bottom portion of the IV curve, caused by the complete consumption of adsorbed reactant gases. These IV curves are shown below (Figures 25 – 26).

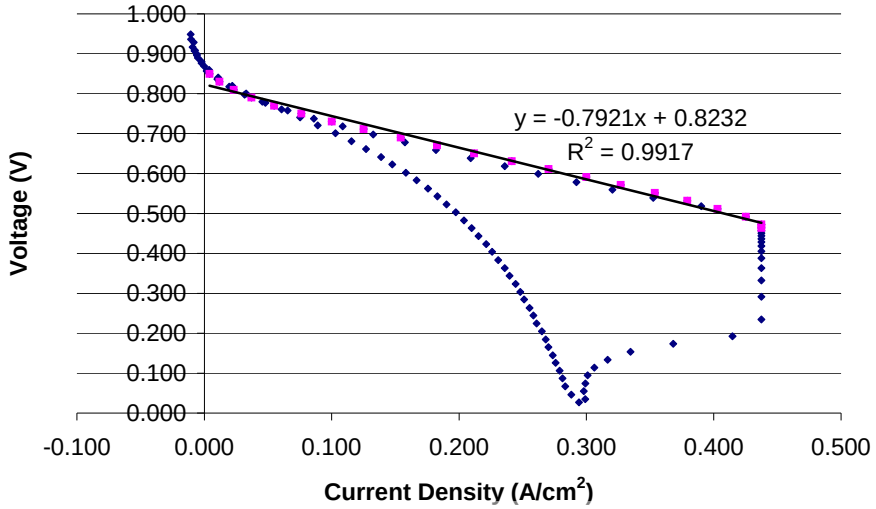


**Figure 25.** Platinum-40 MEA #2 at $60^0$ C, 12.0 ml/min $H_2$, 6.0 ml/min $O_2$

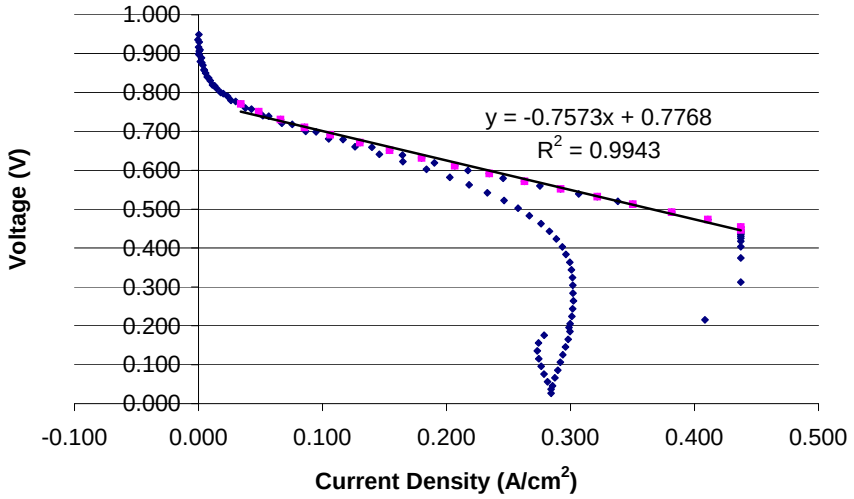


**Figure 26.** Platinum-50 MEA #1 at $60^0$ C, 12.0 ml/min $H_2$, 6.0 ml/min $O_2$

There are far fewer MEAs that displayed this phenomenon at this condition than at the low temperature, high relative humidity testing condition. Therefore, the increased flow rates of both reactant gases must play a role in the phenomenon. The sharp dip in the potential is caused by the consumption of the adsorbed reactant gases and the temporary lack of adsorbed reactant gases to fuel the reaction. Therefore, it makes sense that this

phenomenon is not observed at the higher flow rates of reactant gases because the reactant gases, and therefore the potential, less frequently "bottom out".

The more likely, and the more frequently observed, behavior of the MEAs at high reactant gas flow rates was the limitation near the mass transfer region of the IV curve due to the limitations of the Arbin instrument. This behavior was exhibited by almost all of the MEAs and thus, in almost every case, the maximum current densities exceeded the limitation set by the instrument (0.437 A/cm$^2$) and can not be displayed on the graph. See Figures 27 – 37.

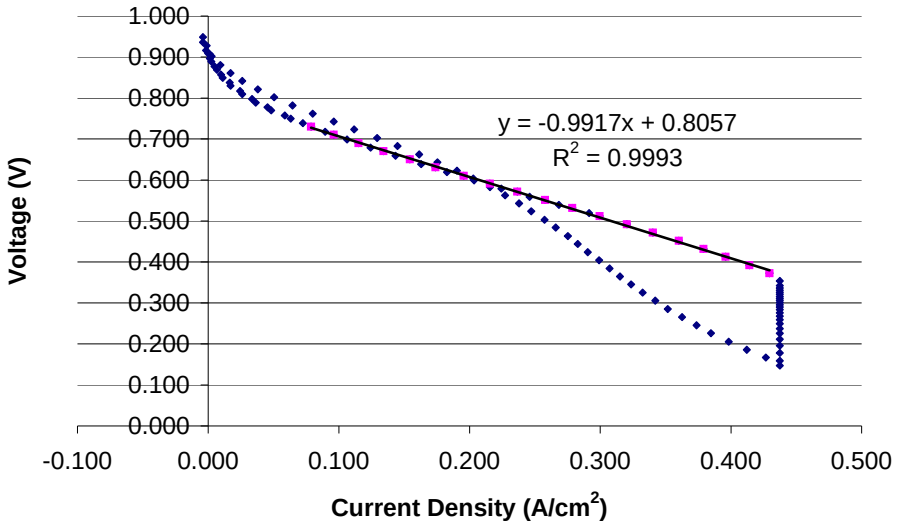


**Figure 27.** Platinum-Platinum MEA #2 at 60$^0$ C, 12.0 ml/min $H_2$, 6.0 ml/min $O_2$

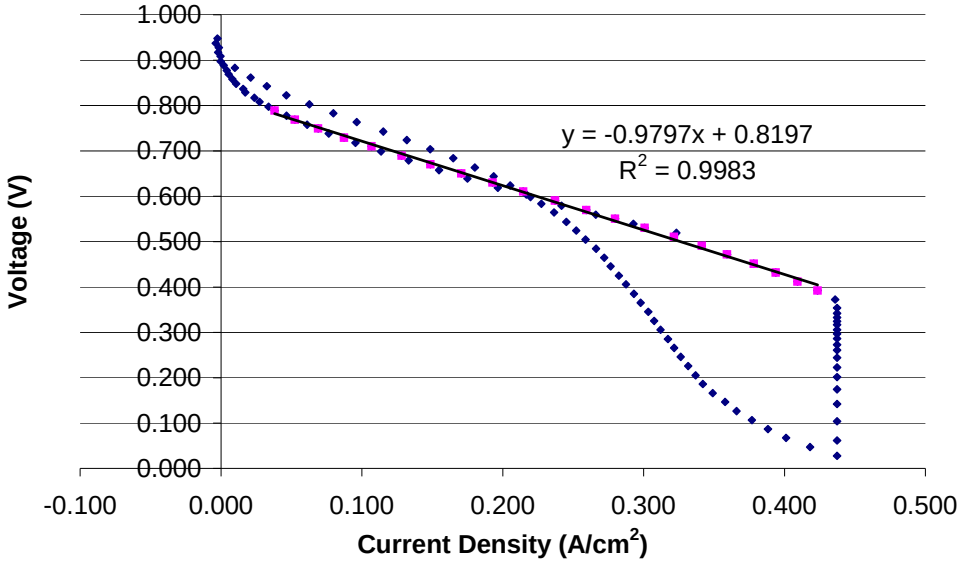


**Figure 28.** Platinum-25 MEA #1 at $60^0$ C, 12.0 ml/min $H_2$, 6.0 ml/min $O_2$

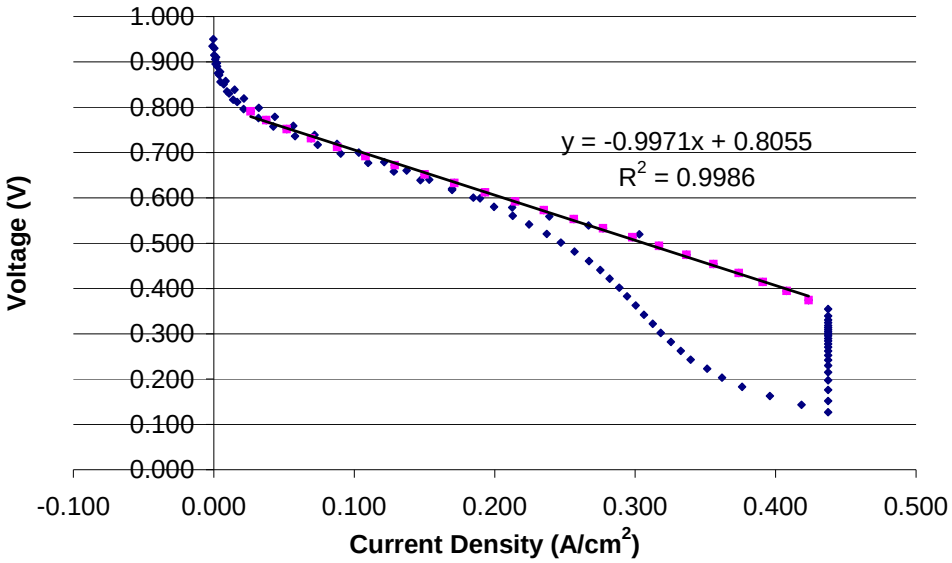


**Figure 29.** Platinum-40 MEA #1 at $60^0$ C, 12.0 ml/min $H_2$, 6.0 $O_2$

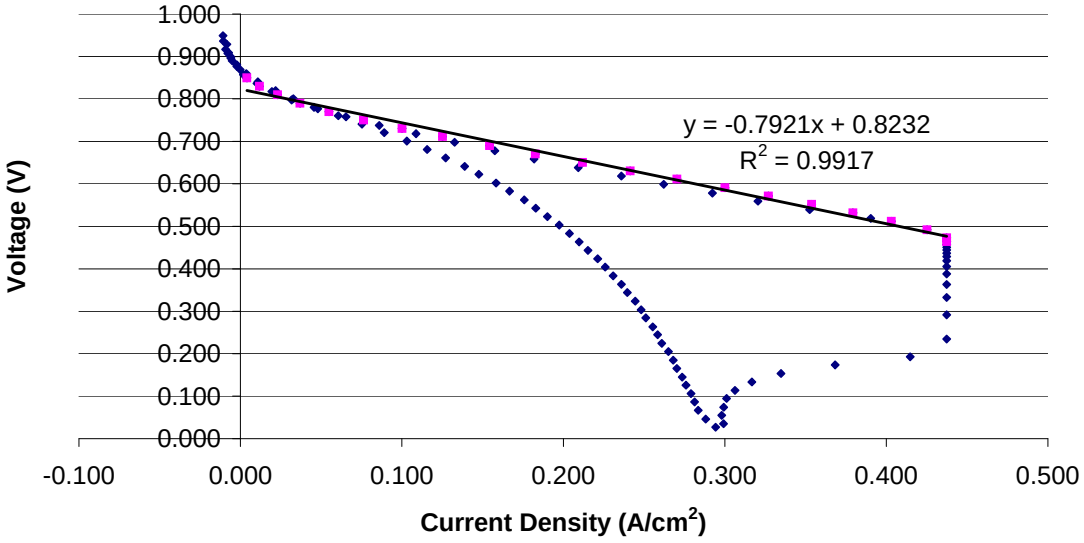


**Figure 30.** Platinum-40 MEA #2 at $60^0$ C, 12.0 ml/min $H_2$, 6.0 $O_2$

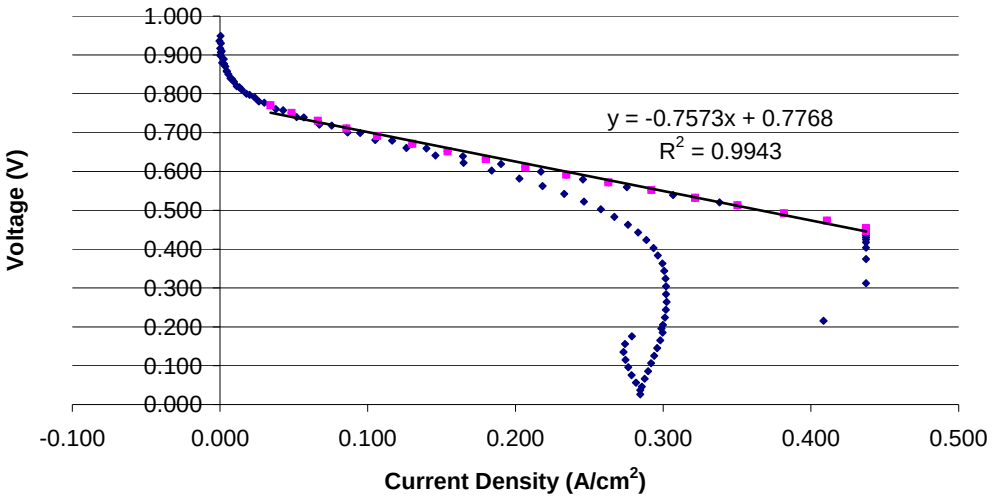


**Figure 31.** Platinum-50 MEA #1 at $60^0$ C, 12.0 ml/min $H_2$, 6.0 $O_2$

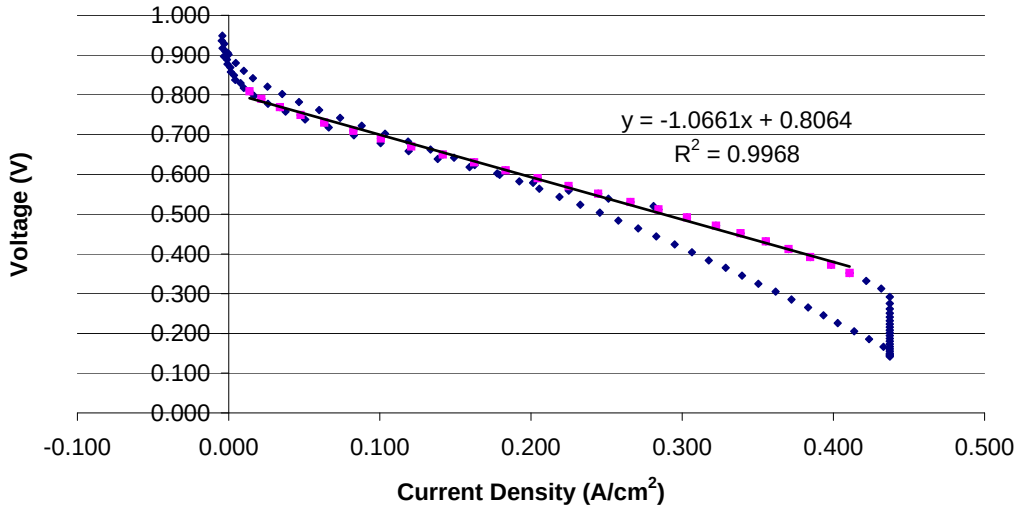


**Figure 32.** Platinum-50 MEA #2 at $60^0$ C, 12.0 ml/min $H_2$, 6.0 $O_2$

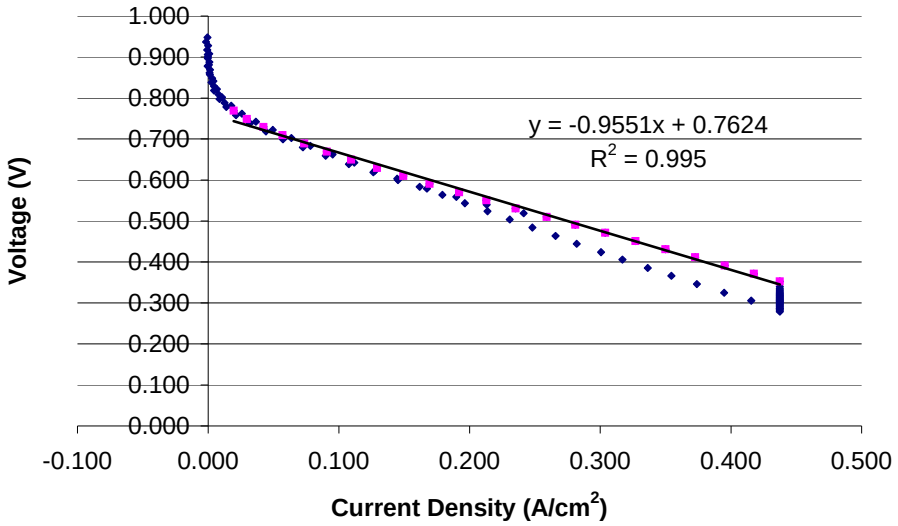


**Figure 33.** Platinum-50 MEA #3 at $60^0$ C, 12.0 ml/min $H_2$, 6.0 $O_2$

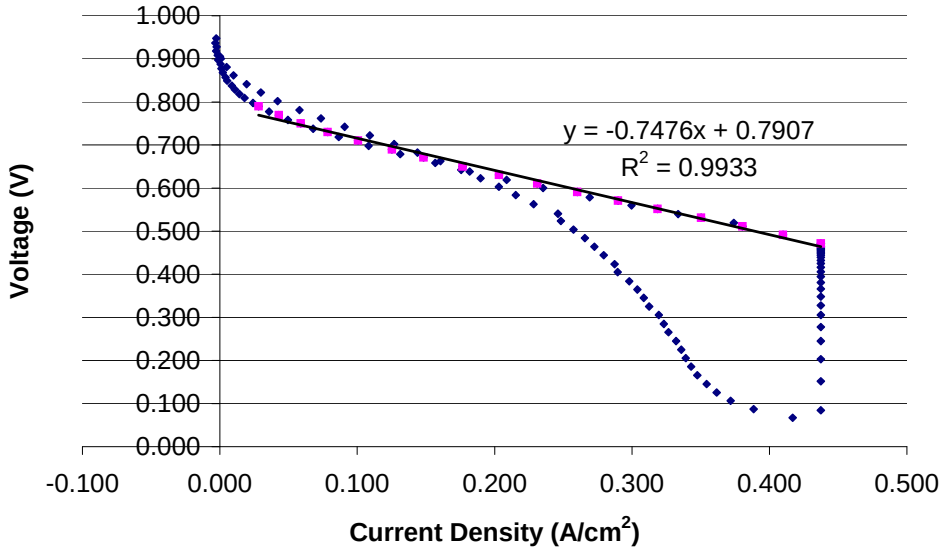


**Figure 34.** Platinum-60 MEA #1 at $60^0$ C, 12.0 ml/min $H_2$, 6.0 $O_2$

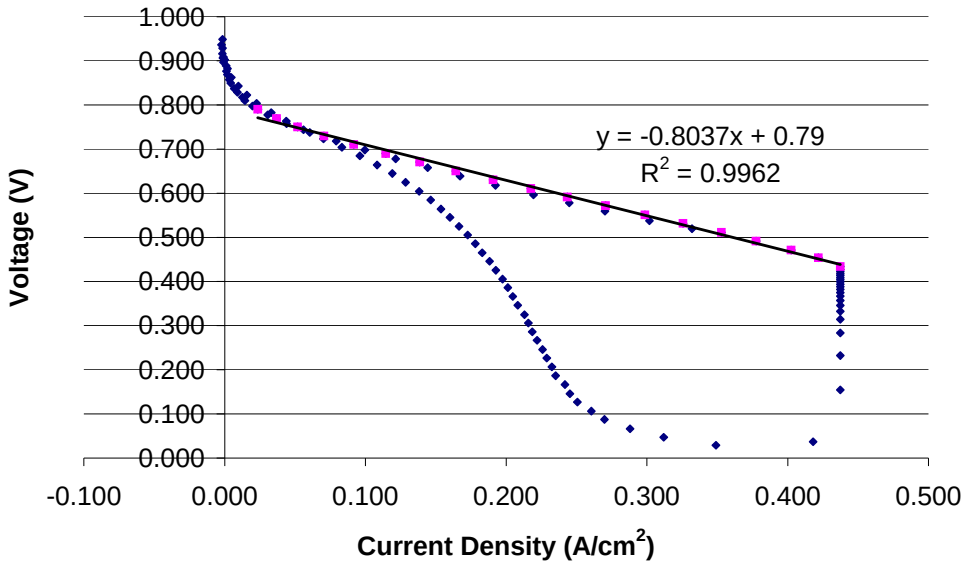


**Figure 35.** Platinum-60 MEA #2 at $60^0$ C, 12.0 ml/min $H_2$, 6.0 $O_2$

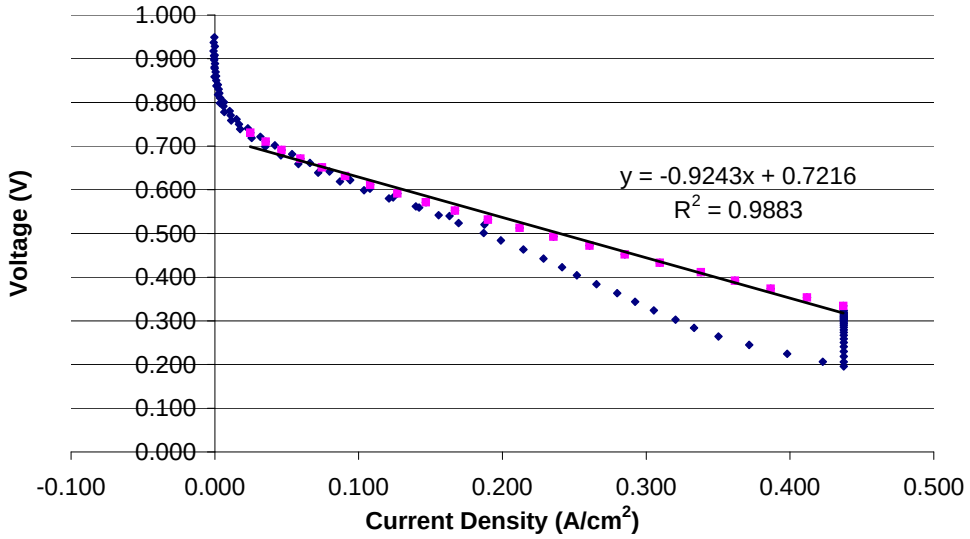


**Figure 36** Platinum-75 MEA #1 at $60^0$ C, 12.0 ml/min $H_2$, 6.0 $O_2$

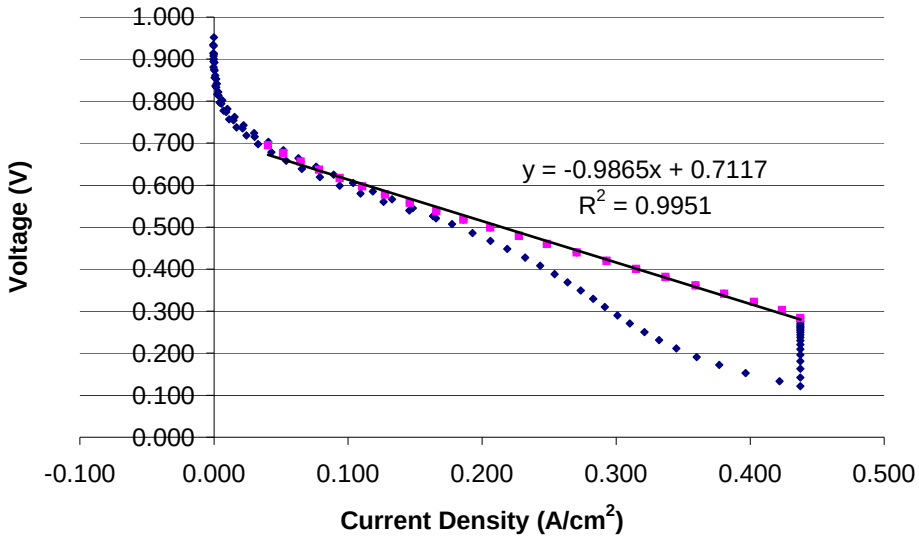


**Figure 37** Platinum-75 MEA #2 at $60^0$ C, 12.0 ml/min $H_2$, 6.0 $O_2$

Not all of the power densities of the MEAs at the low temperature, low relative humidity exceeded the power densities at the low temperature, high relative humidity condition. However, it is clear from the above graphs that the maximum current density was met far more frequently at the low relative humidity than at the high relative humidity condition. This can be explained by the increase in flow rates of the reactant gases and the subsequent affect on the catalytic activity of the combinatorial catalyst layer.

The power densities at the high temperature testing conditions were significantly poorer due to the performance requirements of the polymer membrane electrolyte. Because the polymer membrane electrolyte must remain sufficiently hydrated in order to act as an ion conductor, the operating temperature is limited by the boiling point of water. The optimal operating temperature of PEMFCs is therefore between 60 and 100 $^0$C. At the higher end of this temperature range performance is negatively affected by the dehydration of the membrane, especially at high flow rates of reactant gases as is the case

at the high temperature, low relative humidity testing condition. See Table 7 (asterisks indicate particularly poor MEA performance in terms of crossover and, in the absence of any data, indicate the failure to create enough potential to complete a test).

| MEA | k | $V_0$ | $w_{max}$ (W/cm$^2$) |
|---|---|---|---|
| Pt #1 | 2.82 | 0.820 | 0.0597 |
| Pt #2 | 0.871 | 0.686 | 0.135 |
| | | **AVG** | **0.0974** |
| | | | |
| 25 #1 | 1.42 | 0.771 | 0.105 |
| 25 #2 | 1.34 | 0.762 | 0.109 |
| | | **AVG** | **0.107** |
| | | | |
| 40 #1 | 2.10 | 0.779 | 0.0722 |
| 40 #2 | 0.886 | 0.781 | 0.172 |
| | | **AVG** | **0.122** |
| | | | |
| 50 #1 | 1.45 | 0.753 | 0.0979 |
| *50 #2* | 3.69 | 0.400 | 0.0108 |
| 50 #3 | 1.41 | 0.745 | 0.0986 |
| | | **AVG** | **0.0983** |
| | | | |
| 60 #1 | 1.31 | 0.733 | 0.103 |
| 60 #2 | 1.14 | 0.756 | 0.126 |
| | | **AVG** | **0.114** |
| | | | |
| 75 #1 | 2.05 | 0.712 | 0.0617 |
| 75 #2 | 2.26 | 0.702 | 0.0547 |
| | | **AVG** | **0.0582** |
| | | | |
| Au #1 | 211 | 0.405 | 0.000190 |
| Au #2 | 3.44 | 0.123 | 0.00110 |
| | | **AVG** | **0.000650** |

**Table 7.** Maximum power densities at $90^0$ C, 12.0 ml/min $H_2$, 6.0 ml/min $O_2$

Once again the power density peaks between combinatorial catalyst compositions of 40 wt. % gold and 60 wt. % gold, with the 40 wt. % gold composition yielding the highest power density. The power density increases with percent weight gold until 40 wt. %, slightly decreases at 50 wt. % gold, and peaks again at 60 wt. % gold, and then decreases

with increasing percent weight gold. Once again, the slight decrease at 50 wt. % gold is not thought to be indicative of a decreasing trend at this composition.

The phenomenon of adsorbed reactant gases being thoroughly consumed resulting in the potential "bottoming-out" only occurred with one MEA at the high temperature, low relative humidity condition – Platinum-40 MEA #2. See Figure 38

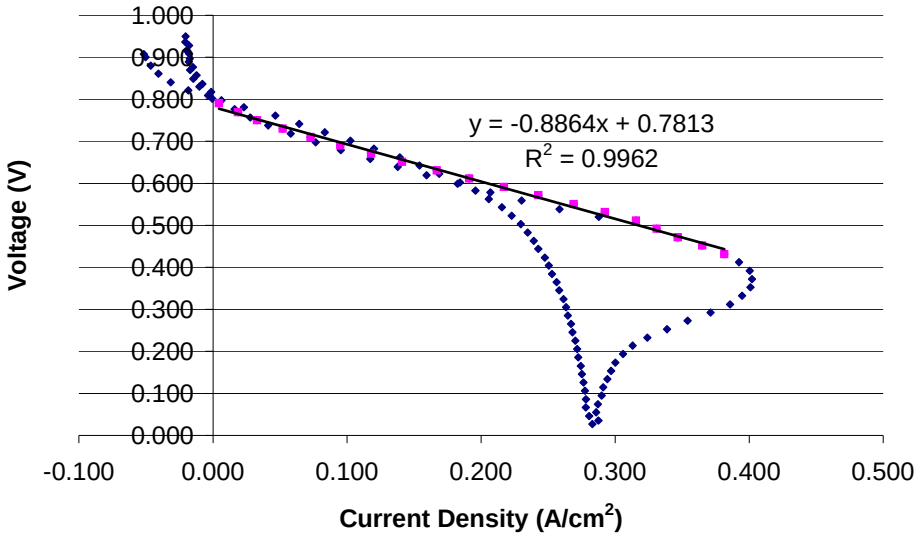


**Figure 38** Platinum-40 MEA #2 at $90^0$ C, 12.0 ml/min $H_2$, 6.0 ml/min $O_2$

The rarity of this phenomenon at this testing condition can be explained by the high flow rate of reactant gases, which prevents the reaction from running out of reactant gases. Furthermore, the high temperature at this testing condition prevents the MEAs from achieving maximum current densities greater than 0.437 A/cm$^2$. Hence, the second phenomenon described above, which involves the sudden drop in potential at 0.437 A/cm$^2$ due to instrument limitations, is not observed at this testing condition for any of the MEAs.

In the case of the high temperature, high relative humidity testing condition, the 40 wt. % gold, 60 wt. % platinum combinatorial catalyst resulted in the highest maximum

power density. The maximum power density increased with increasing percent weight gold until the 40 wt. % composition, then slightly decreased with increasing percent weight gold, drastically decreasing at gold weight percentages greater than 60%. See Table 8 (asterisks indicate particularly poor performance in terms of crossover or the lack of test results due to insufficient potential).

| **MEA** | **k** | **$V_0$** | **$w_{max}$ ($W/cm^2$)** |
|---|---|---|---|
| Pt #1 | 1.357 | 0.813 | 0.122 |
| *Pt #2* | 0.936 | 0.709 | 0.1342 |
| | | **AVG** | **0.122** |
| | | | |
| 25 #1 | 1.67 | 0.806 | 0.09732 |
| 25 #2 | 1.77 | 0.773 | 0.0844 |
| | | **AVG** | **0.0909** |
| | | | |
| 40 #1 | *** | *** | *** |
| 40 #2 | 1.09 | 0.798 | 0.147 |
| | | **AVG** | **0.147** |
| | | | |
| 50 #1 | *** | *** | *** |
| *50 #2* | 1.31 | 0.764 | 0.111 |
| 50 #3 | 1.48 | 0.776 | 0.101 |
| | | **AVG** | **0.106** |
| | | | |
| 60 #1 | 1.28 | 0.755 | 0.111 |
| 60 #2 | 1.52 | 0.760 | 0.0951 |
| | | **AVG** | **0.103** |
| | | | |
| 75 #1 | 1.48 | 0.692 | 0.0810 |
| 75 #2 | 1.97 | 0.706 | 0.0632 |
| | | **AVG** | **0.0721** |
| | | | |
| Au #1 | 7.80 | 0.439 | 0.00618 |
| Au #2 | 72.0 | 0.0349 | 4.23 E-06 |
| | | **AVG** | **0.00309** |

**Table 8.** Maximum power densities at $90^0$ C, 8.0 ml/min $H_2$, 4.0 ml/min $O_2$

The power densities at the high temperature, high relative humidity testing condition were, for every catalyst combination except the 60 wt. % gold, 40 wt. % platinum

combination, higher than those at the high temperature, low relative humidity testing condition. This difference can be attributed to further dehydration of the polymer membrane at the low relative humidity (high reactant gas flow rate) condition. The higher power density for the 60 wt. % gold, 40 wt. % platinum combination at the low relative humidity (high reactant gas flow rate) condition, as compared to the power density for this combinatorial catalyst at the high relative humidity condition, suggests that the catalytic activity of the high performance catalyst combination had more of an affect on the power density than did the dehydration of the membrane.

The "bottoming-out" of the potential due to a lack of adsorbed reactant gases to feed the reaction occurred for only three of the MEAs at the high temperature, high relative humidity testing condition. See Figures 39– 41

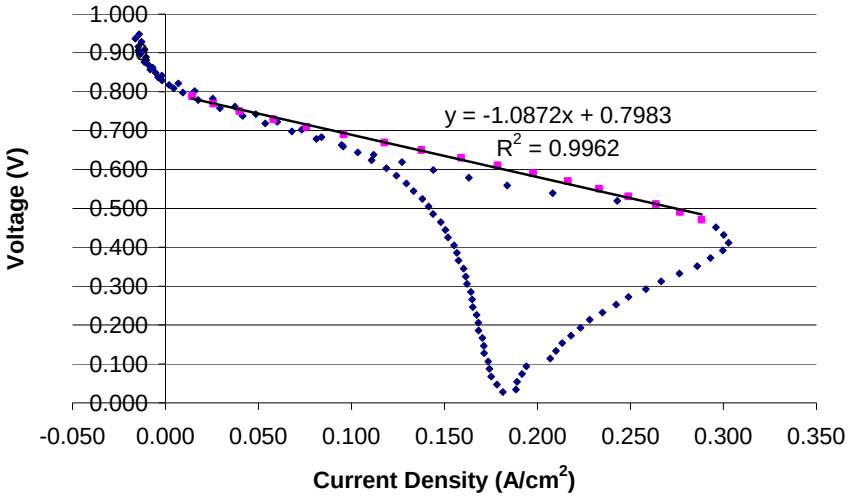


**Figure 39.** Platinum-40 MEA #2 at $90^0$ C, 8.0 ml/min $H_2$, 4.0 ml/min $O_2$

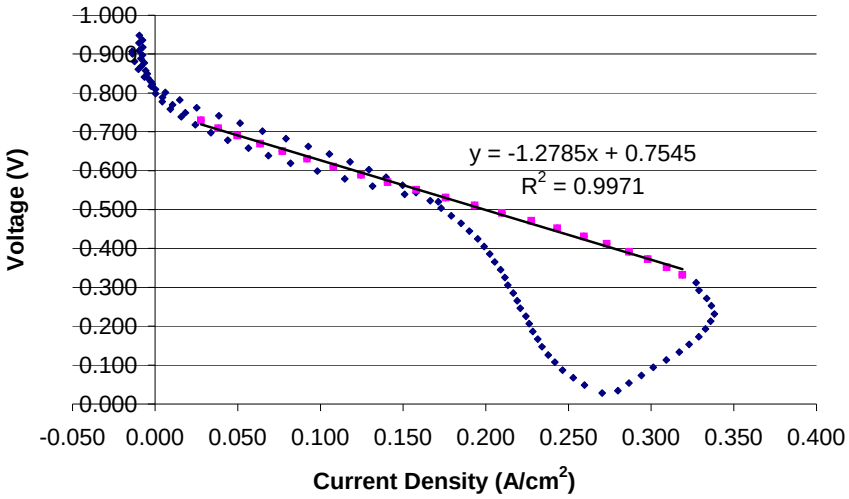


**Figure 40.** Platinum-60 MEA #1 at $90^0$ C, 8.0 ml/min $H_2$, 4.0 ml/min $O_2$

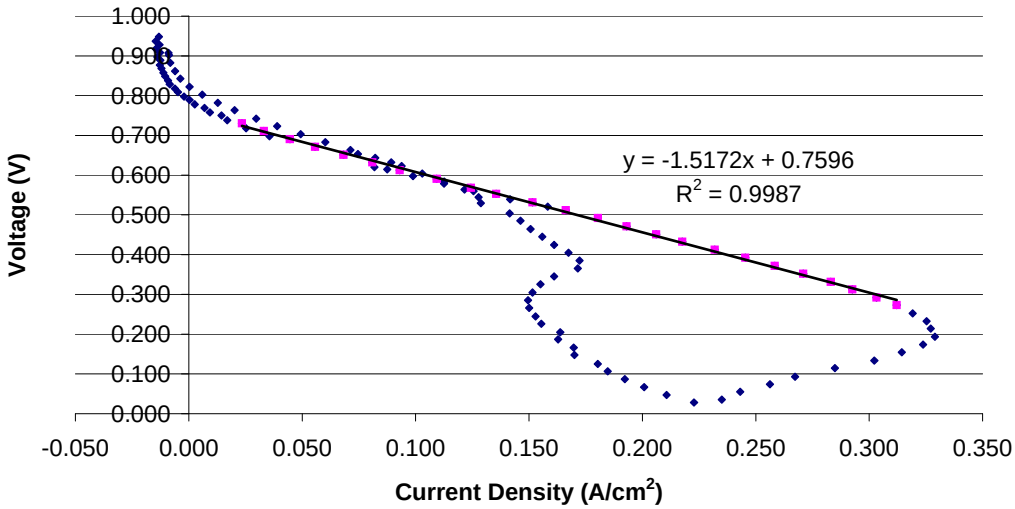


**Figure 41.** Platinum-60 MEA #2 at $90^0$ C, 8.0 ml/min $H_2$, 4.0 ml/min $O_2$

This phenomenon occurred only slightly more frequently at the high temperature, high relative humidity testing condition than at the high temperature, low relative humidity testing condition, which can be explained by the fact that there is less mass flow of reactant gases at the high temperature, high relative humidity testing condition and therefore "bottoming-out" occurs more often. However, because maximum current densities (a measure of reaction rate) are smaller at the higher temperature, less reactant gas mass flow is needed to fuel the reaction. Therefore, the "bottoming-out" phenomenon occurs much less frequently at the high temperature testing conditions than at the low temperature testing conditions. Interestingly enough, although the 100 wt. % platinum cathode catalyst resulted in a lower power density than the optimum combinatorial catalyst at the high temperature, high relative humidity testing condition, it still resulted in the largest maximum current density (0.437 A/cm$^2$, the maximum current density instrument limit). See Figure 42.

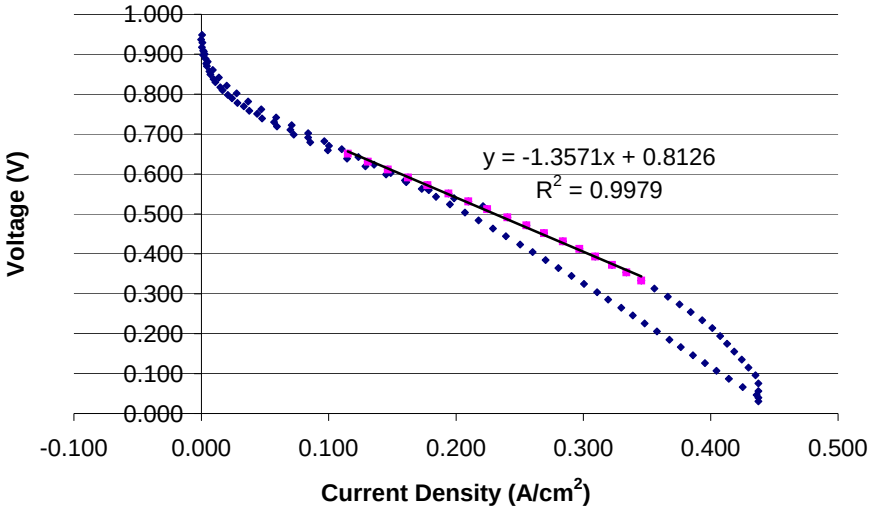


**Figure 42.** Platinum-Platinum MEA #1 at $90^0$ C, 8.0 ml/min $H_2$, 4.0 ml/min $O_2$

This suggests that different trends may be observed in the maximum current density that for the maximum power density.

The maximum current densities, as shown in Table 9, vary not only with cathode catalyst combination but also with testing condition.

| | $60^0$ C, 8.0 ml/min $H_2$, 4.0 ml/min $O_2$ | $60^0$ C, 12.0 ml/min $H_2$, 6.0 ml/min $O_2$ | $90^0$ C, 12.0 ml/min $H_2$, 6.0 ml/min $O_2$ | $90^0$ C, 8.0 ml/min $H_2$, 4.0 ml/min $O_2$ | **AVG** |
|---|---|---|---|---|---|
| Pt #1 | **0.437** | 0.291 | 0.146 | **0.437** | **0.328** |
| Pt #2 | **0.437** | **0.437** | 0.354 | 0.082 | |
| 25 #1 | 0.399 | **0.437** | 0.334 | 0.243 | **0.339** |
| 25 #2 | 0.415 | 0.33 | 0.336 | 0.221 | |
| 40 #1 | **0.437** | **0.437** | 0.224 | *** | **0.380** |
| 40 #2 | **0.437** | **0.437** | 0.402 | 0.303 | |
| 50 #1 | **0.437** | **0.437** | 0.374 | *** | **0.409** |
| 50 #2 | 0.317 | **0.437** | 0.114 | 0.266 | |
| 50 #3 | **0.437** | **0.437** | 0.381 | 0.349 | |
| 60 #1 | **0.437** | **0.437** | 0.408 | 0.338 | **0.405** |
| 60 #2 | 0.436 | **0.437** | 0.415 | 0.329 | |
| 75 #1 | **0.437** | **0.437** | 0.284 | 0.326 | **0.355** |
| 75 #2 | 0.416 | **0.437** | 0.249 | 0.252 | |
| Au #1 | 0.14 | 0.025 | 0.002 | 0.066 | **0.155** |
| Au #2 | 0.164 | 0.193 | 0.03 | 0.001 | |
| | | | | | |
| **AVG** | **0.386** | **0.402** | **0.289** | **0.247** | |
| | | | | | |

**Table 9.** Maximum Current Densities ($A/cm^2$)

As discussed previously, the maximum current density instrument limit, 0.437 $A/cm^2$, is met more frequently at the low temperature than at the high temperature testing conditions and met most frequently at the low temperature, high flow rate (low humidity testing condition). The increase in performance of the MEAs at the low temperature, high flow rate as compared to the performance at the low temperature, low flow rate condition defies the theory that dehydration of the polymer membrane leads to poorer performance. This is due to stoichiometry and also suggests that an increase in flow rate affects the adsorption of the reactant gases on the electrodes and alters the catalytic activity. The

average maximum current density at both low temperature testing conditions is significantly higher than the averages at the high temperature testing conditions due to dehydration of the polymer membrane and possible affects of temperature on the catalytic activity of the combinatorial catalysts. The maximum current densities at the higher temperature testing conditions do not reach the maximum current density limit because of their relatively poor performance. However, once again, the high temperature, high flow rate condition leads to a higher average maximum current density than the high temperature, low flow rate condition, suggesting that dehydration of the membrane is not the only factor affecting maximum current density.

Preliminary results indicate that the hypothesis concerning possible synergies between gold and platinum, the benefits of gold on the cathode catalyst layer, and the respective increase in efficiency of the catalyst layer is correct. However simple measurements of rates (for example, exchange-current densities) and, therefore, also measurements of power densities, are evidently fraught with secondary factors, which are not those connected with electronic bonding and the geometric effects of catalysts.[lxxii] It is necessary to positively determine if temperature or relative humidity has any effect on catalyst behavior. It is also necessary to determine if certain phenomena such as "bottoming-out" are due to catalytic affects or testing conditions or both. If changes in the shape of IV curves can be directly linked to catalytic affects it could be possible to determine the mechanisms involved in the catalytic activity and examine the validity of the observed patterns. Assuming that the observed patterns are valid reflections of the efficiency of the catalyst layer, the 40 wt. % gold/60 wt. % platinum combinatorial catalyst at the cathode offers a 47%, 54%, 25%, and 20% improvement over the platinum

catalyst at the cathode at the low temperature/high humidity, low temperature/low humidity, high temperature/low humidity, high temperature/high humidity testing conditions respectively. The 60 wt. % gold/40 wt. % platinum combinatorial catalyst at the cathode offers a 46%, 66%, and 17% improvement over the platinum catalyst at the cathode at the low temperature/high humidity, low temperature/low humidity, high temperature/low humidity testing conditions respectively. The largest improvement over platinum catalyst was seen with the 60 wt. % gold/40 wt. % platinum combinatorial catalyst at the low temperature/low relative humidity testing condition.

# V. CONCLUSION

Fuel cells are extremely efficient and nonpolluting electrochemical energy converters that convert fuel (usually hydrogen) directly into electricity via the oxidation of hydrogen and reduction of oxygen. Hydrogen enters the fuel cell at the anode and is adsorbed and stripped of its electrons. The protons move through the electrolyte and the electrons move through an external circuit to create electricity. Oxygen enters the fuel cell at the cathode where it combines with protons and electrons to form either water or hydrogen peroxide. Because fuel cells directly convert the fuel into energy they do not underlie the limitations of the Carnot cycle. Theoretical fuel cell efficiency is instead equal to the ratio between the useful energy output (the Gibbs free energy) and the total energy input contained in the fuel (the enthalpy). The theoretical fuel cell efficiency is equal to 83%. However, the practical energy efficiency ranges between 35 and 70% as compared to the practical energy efficiency of heat engines, which is well below 30%. Fuel cell technology also offers the potential for lowering or eliminating emissions, particularly when hydrogen is used as the fuel. Currently the cost of fuel cells fails to compare to other energy technologies and it is therefore necessary to increase the efficiency of fuel cells while decreasing the cost. The current primary areas of fuel cell development fall under two categories: the development of a hydrogen infrastructure and the mass production of efficient MEAs. Because the reactions involved in producing electricity in a fuel cell occur at the catalyst layer of the electrode at the three phase boundary it is this catalyst layer that offers the largest potential for efficiency improvement.

PEMFCs operate at a lower temperature (60 –$100^0$ C) due to the use of a thin proton conductive polymer membrane electrolyte and have a higher power density as well as more design flexibility and convenience than other types of fuel cells. They are therefore the most likely to be used in automobiles and offer significant emissions advantages. The polymer membrane electrolyte in a PEMFC is sandwiched between two porous, electrically conductive electrodes, which are made out of carbon cloth or carbon fiber paper. At the interface between the electrodes and the polymer membrane there exists a catalyst layer, which is typically platinum supported on carbon. The electrochemical reactions take place at this interface. The membrane electrode assembly is placed between the collector/separator plates, which collect and conduct electrical current. When PEMFC technology was first invented in the 1960s it required pure hydrogen and oxygen and very high precious metal loadings, which made it impractical for terrestrial applications. However, technical breakthroughs between 1985 and 1995 led to the lowering of precious metal loadings, effective approaches to operation with air and impure hydrogen fuel, and resolution of water management issues.

Polymer membrane electrolytes are comprised of a hydrophobic Teflon-like backbone and a hydrophyllic sulphonic acid side chain. The relative hydrophobicity and hydrophyllicity contribute to the water management issues in a PEMFC. The perfluorinated ionomer membranes known under the trade name of Nafion have been found to have favorable chemical, mechanical, and thermal properties along with high proton conductivity when sufficiently hydrated. Furthermore, the solid state perfluorinated acid electrolyte environment offers significant advantages over phosphoric acid for oxygen reduction. The polymer exchange membrane should have high proton

conductivity and immobilized anions. It should be insoluble in water but water should be soluble in the membrane. The membrane should be impermeable to hydrogena nd oxygen (low crossover). There should exist structural, chemical, thermal and electrochemical stability as well as tolerance to impurities. The membrane should exhibit swift water transport and reversible hydration. In addition to managing the hydration of the cell to maximize the efficiency of the polymer membrane, it is also necessary to maximize the efficiency of the electrode structure – specifically the catalyst layer.

The electrode structure and catalyst layer can be improved in several ways. As early as the mid-1800s, it was discovered that a porous electrode structure with high surface area could increase the area of the region in which the chemical reactions take place on the electrode surface. It was also determined that coating the catalyst layer with a thin film of electrolyte led to better performance. The next early developments included developing a non-conducting porous matrix to hold the liquid electrolyte and using a powdered electrocatalyst in the form of platinum black. A rough electrode surface can increase the current under the activation control at any overpotential, however, diffusion rates are not greatly enhanced unless the depths of roughness are at least of the order of magnitude of diffusion-layer thickness. The use of porous electrode material does increase the rate of diffusional processes, thereby facilitating mass transfer to reactant sites and increasing the overall efficiency of the fuel cell. The gas diffusion layer, which typically consists of a thin layer of carbon particles on the surface of the porous carbon substrate, must be optimized so that reactant gases can diffuse but also so that water does not accumulate within the pores. The diffusion layer must be electrically and thermally conductive and provide mechanical support, electrical contact, optimal distribution of

reactant gases, and a pore structure suitable for the removal of water. In order to satisfy these requirements, a catalyst slurry ink is applied to the gas diffusion layer or the membrane itself.

The catalyst plays a role in three main processes in electrochemical reactions: adsorption, charge transfer, and surface reactions. The catalyst's role in adsorption and surface reactions makes geometric and electronic factors important in the catalysis of the reaction but the charge transfer step also makes the potential at the metal-solution interface an additional factor for electrochemical reactions. Especially in PEMFCs, the platinum catalyst loading must be significantly reduced before the technology can be cost competitive and market introduction can be effected on a broad basis. In order to increase the efficiency of the catalyst layer and thereby decrease platinum loadings the surface area of the catalyst layer must be increased. This can be accomplished either by roughening the surface of the membrane or incorporating some ionomer in the catalyst layer. Dispersing platinum on carbon black also leads to a higher platinum surface area and lower platinum loadings. Noble metals have the highest catalytic activity for the hydrogen-evolution reaction and other transition metals have intermediate catalytic power. Alloys of noble metals with other metals can also be used as catalysts but the surface structure is altered by alloying and may lead to poorer performance. Although platinum is the most commonly used catalyst in PEMFCs, its strong adsorptive characteristics lead to poor performance at the cathode for the oxygen-reduction reaction.

The slowness of the oxygen-reduction reaction is the principal problem in hydrogen-oxygen fuel cells. Even at the lowest current density, there is a loss in potential of the oxygen electrode from the reversible electrode potential by 0.2 to 0.3 volt which

results in a 25% decrease in conversion efficiency. If it were possible to make the ORR increasingly reversible, fuel cells could approach theoretical efficiencies. Under typical conditions at the platinum catalyst surface, the oxygen reduction intermediate species share the electrode surface with platinum oxide and or hydroxide compounds as well as other adsorbed species. Carbon supported platinum alloys have been shown to be more active and stable as oxygen reduction catalyst but still lead to a high adsorptive character that hinders the oxygen reduction reaction.

It has been hypothesized that using a combinatorial catalyst of gold, which does not have the adsorptive character that hydrogen does, and platinum could mitigate the problem of adsorption of oxygen, intermediates, and impurities at the cathode and thereby facilitate the chemical reaction involving the recombination of oxygen with protons and electrons in order to form water. Gold is also slightly less expensive than platinum. E-TEK gives a price quote for 20% gold on Vulcan XC-72 (carbon support) equal to $26.61/g compared to $31.62/g for 20% platinum on Vulcan XC-72. Gold and palladium alloys have been investigated as alternatives to a solid platinum catalyst with disappointing results. There was found to be a decrease in current density with increase of gold composition. However, enhanced activity was observed with the use of gold single crystal surfaces when covered by thin palladium layers. Gold, having no unpaired d-electrons, does not adsorb oxygen and has a high potential for oxide formation. It is probable that by alloying gold with other metals, the surface characteristics are changed and the ability to adsorb various intermediates, reactants, and impurities increases, thereby negating the benefits of gold as a catalyst.

By using a slurry combination of platinum and gold, instead of an alloy, it is possible to take advantage of the benefits of platinum's high adsorption activity and catalytic activity as well as gold's lack of adsorption activity. Combinatorial catalyst slurries were created by sonicating a total of 0.050 g 20% platinum on carbon (by weight) and 20% gold on carbon (by weight) with approximately 10 g isopropanol for more than thirty minutes. Each slurry was created with a specific weight ratio of platinum to gold in order to determine the appropriate ratio for optimizing overall MEA performance. The percent weights of gold/platinum tested were: 0/100, 25/75, 40/60, 50/50, 60/40, 75/25, and 100/0. Each of these slurries was applied to the cathode while the anode was coated with a 100% platinum slurry. Two MEAs were produced for each combinatorial cathode catalyst in order to confirm that results were reproducible. Each MEA was then tested at both a low temperature and a high temperature and a low relative humidity (high reactant gas flow rate) and high relative humidity (low reactant gas flow rate). Three CV curves were obtained for each MEA at each testing condition. Maximum power densities were calculated for one CV curve for each MEA at each testing condition and compared with one another to determine the best possible combinatorial catalyst and testing condition.

At both low temperature testing conditions and the high temperature, low relative humidity testing condition, the power density increased with gold composition and peaked at the 40 wt. % gold/60 wt. % platinum combination, decreased at the 50/50 wt. % combination, peaked again at the 60 wt. % gold/40 wt. % platinum combination, then decreased with increasing gold composition. At the high temperature, high relative humidity testing condition, the power density increased with gold composition, peaking at a 40 wt. % gold combination, then decreased with increasing gold composition. The

power densities were generally lower at the high temperature testing conditions than at the low temperature testing conditions due to dehydration of the membrane. The low relative humidity testing conditions, however, because they involved a larger reactant gas flow rate, resulted in high power densities and higher maximum current densities than the high relative humidity testing conditions. A drastic dip in the voltage occurred on many of the graphs and is thought to be a representation of the complete coating of the electrode with adsorbed anions. These adsorbed anions are then gradually consumed by the reaction and the potential gradually increases. Many of the graphs do not show a mass transfer regime due to the maximum current limitations of the testing software. The best results were obtained with the 60 wt. % gold/40 wt. % platinum combinatorial cathode catalyst at the low temperature/low relative humidity testing condition, which showed a 66% improvement over the platinum cathode catalyst at the same testing condition. PEMFCs, with their high power density and low operating temperature, offer a viable solution for reducing emissions and shifting reliance on fossil fuels over to a hydrogen-based economy but only if their cost can be reduced and a hydrogen infrastructure can be built. Both of these tasks are difficult at best. However, by tackling the problem of slow oxygen-reduction kinetics at the cathode and increasing the efficiency of the catalyst layer, it is possible to decrease platinum loadings and bring down the cost of fuel cell manufacturing. Although platinum has been shown to be an effective catalyst for PEMFCs, its highly adsorptive character makes it an inefficient catalyst for the oxygen reduction reaction and contributes to the slow reaction kinetics at the cathode. By incorporating some gold in the catalyst layer at the cathode this adsorptive character can be weakened, thereby promoting the oxygen reduction reaction and increasing the

efficiency of the fuel cell. Although significant cost reduction and hydrogen infrastructure development lie between current technologies and a fuel cell powered future, the increase in efficiency of the catalyst layer at the cathode through the addition of gold proves to be a step in the right direction.

[i] Barbir, Frano. PEM Fuel Cells: Theory and Practice. Elsevier Academic Press (2005): Burlington, MA. pgs. 20-21.
[ii]Barbir, Frano. pg. 39.
[iii]Hamnett, A. "The components of an electrochemical cell." *Handbook of Fuel Cells: Fundamentals, Technology, and Applications,* Edited by Wolf Vielstich, Arnold Lamm, and Hubert A. Gasteiger. Volume 1: *Fundamentals and survey of systems*. © 2003 John Wiley & Sons Ltd. pg. 6.
[iv] Oniciu, Liviu. Fuel Cells. Abacus Press (1976): Tunbridge Wells, Kent. Pg. 31.
[v] Bockris & Srinivasan. Fuel Cells: Their Electrochemistry. McGraw-Hill Book Company (1969): New York, New York. pg. 35.
[vi] Bockris & Srinivasan. Pg. 35
[vii]Barbir, Frano. Pg. 12.
[viii] *Handbook of Fuel Cells: Fuel Cell Technology and Applications.* Edited by Wolf Vielstich, Arnold Lamm, and Hubert A. Gasteiger. Volume 3: *Fuel Cell Technology and Applications, Part 1.* © 2003 John Wiley & Sons Ltd. pg. xvi.
[ix] Ogden, J. M. "Alternative fuels and prospects – Overview." *Handbook of Fuel Cells: Fuel Cell Technology and Applications.* Edited by Wolf Vielstich, Arnold Lamm, and Hubert A. Gasteiger. Volume 3: *Fuel Cell Technology and Applications, Part 1.* © 2003 John Wiley & Sons Ltd. pg. 9.
[x] Ogden, J. M. pg. 5.
[xi] Ogden, J. M. pgs. 10
[xii] Ogden, J. M. pg. 13.
[xiii] Ogden, J. M. pgs. 10
[xiv] *Handbook of Fuel Cells: Fuel Cell Technology and Applications.* Edited by Wolf Vielstich, Arnold Lamm, and Hubert A. Gasteiger. Volume 3: *Fuel Cell Technology and Applications, Part 1.* © 2003 John Wiley & Sons Ltd. pg. 121.
[xv] Barbir, Frano. pgs. 6-9.
[xvi] Ogden, J. M. pgs. 6-7.
[xvii] *Handbook of Fuel Cells: Fuel Cell Technology and Applications*. pg. xvii.
[xviii] "SERC: The PEM Fuel Cell Schematic." The Schatz Energy Research Center. <http://www.humboldt.edu/~serc/schematic.html>
[xix] Doyle, M. and Rajendran, G. "Perfluorinated Membranes." *Handbook of Fuel Cells: Fuel Cell Technology and Applications.* Edited by Wolf Vielstich, Arnold Lamm, and Hubert A. Gasteiger. Volume 3: *Fuel Cell Technology and Applications, Part 1.* © 2003 John Wiley & Sons Ltd. pg. 352.
[xx] Paddison, S. J. "First Principles modeling of sulfonic acid based ionomer membranes." *Handbook of Fuel Cells: Fuel Cell Technology and Applications.* Edited by Wolf Vielstich, Arnold Lamm, and Hubert A. Gasteiger. Volume 3: *Fuel Cell Technology and Applications, Part 1.* © 2003 John Wiley & Sons Ltd. pg. 398.
[xxi] Wainright, J. S., Litt, M. H., and Savinell, R. F. "High-Temperature Membranes". *Handbook of Fuel Cells: Fuel Cell Technology and Applications.* Edited by Wolf Vielstich, Arnold Lamm, and Hubert A. Gasteiger. Volume 3: *Fuel Cell Technology and Applications, Part 1.* © 2003 John Wiley & Sons Ltd. pg. 436.
[xxii] Wainright, J. S., Litt, M. H., and Savinell, R. F. pg. 436.
[xxiii] Paddison, S. J. pg. 398-399.
[xxiv] Lin, J. –C., Kunz, H. R., and Fenton, J. M. "Membrane/electrode additives for low-humidification operation." *Handbook of Fuel Cells: Fuel Cell Technology and Applications.* Edited by Wolf Vielstich, Arnold Lamm, and Hubert A. Gasteiger. Volume 3: *Fuel Cell Technology and Applications, Part 1.* © 2003 John Wiley & Sons Ltd. pg. 456.
[xxv] S. Mukerjee and S. Srinivasan. "$O_2$ reduction and structure-related parameters for supported catalysts." *Handbook of Fuel Cells – Fundamentals, Technology and Applications*, Edited by Wolf Vielstich, Hubert

A. Gasteiger, Arnold Lamm. Volume 2: *Electrocatalysis*. © 2003 John Wiley & Sons, Ltd. ISBN: 0-471-49926-9. pg. 504.

[xxvi] Kocha, S. S. "Principles of MEA preparation." *Handbook of Fuel Cells: Fuel Cell Technology and Applications.* Edited by Wolf Vielstich, Arnold Lamm, and Hubert A. Gasteiger. Volume 3: *Fuel Cell Technology and Applications, Part 1.* © 2003 John Wiley & Sons Ltd. pg. 538.

[xxvii] Bockris & Srinivasan. Pg. 230-232.

[xxviii] Bockris & Srinivasan. Pg. 230-232.

[xxix] Bockris & Srinivasan. Pg. 289.

[xxx] Fuel Cells. *A Symposium held by the Gas and Fuel Division of the American Chemical Society at the 136th National Meeting in Atlantic City*, Vol 1. Edited by G. J. Young. Reinhold Publishing Corporation (1960): New York, New York. pg 24.

[xxxi] Vielstich, W. "What is electrocatalysis?" *Handbook of Fuel Cells – Fundamentals, Technology and Applications*, Edited by Wolf Vielstich, Hubert A. Gasteiger, Arnold Lamm. Volume 2: *Electrocatalysis*. © 2003 John Wiley & Sons, Ltd. ISBN: 0-471-49926-9. pg. 10.

[xxxii] Bockris & Srinivasan. Pg. 300.

[xxxiii] Bockris & Srinivasan. Pg. 289.

[xxxiv] Bockris & Srinivasan. Pg. 301-304.

[xxxv] Bockris & Srinivasan. Pg. 315-316.

[xxxvi] Bockris & Srinivasan. Pg. 309.

[xxxvii] Bockris & Srinivasan. Pg. 312-314.

[xxxviii] Bockris & Srinivasan. Pg. 317-321.

[xxxix] Bockris & Srinivasan. Pg. 317-321.

[xl] Bockris & Srinivasan. Pg. 317-321.

[xli] C. Sanchez and E. Leiva. "Understanding electrocatalysis: From reaction steps to first-principles calculations." *Handbook of Fuel Cells – Fundamentals, Technology and Applications*, Edited by Wolf Vielstich, Hubert A. Gasteiger, Arnold Lamm. Volume 2: *Electrocatalysis*. © 2003 John Wiley & Sons, Ltd. ISBN: 0-471-49926-9. pg. 30.

[xlii] Vielstich, W. pg. 3.

[xliii] Bockris & Srinivasan. Pg. 292.

[xliv] Bockris & Srinivasan. pg. 412.

[xlv] Bockris & Srinivasan. pg. 415.

[xlvi] Bockris & Srinivasan. pg. 417.

[xlvii] C. Sanchez and E. Leiva. "Catalysis by UPD metals." *Handbook of Fuel Cells – Fundamentals, Technology and Applications*, Edited by Wolf Vielstich, Hubert A. Gasteiger, Arnold Lamm. Volume 2: *Electrocatalysis*. © 2003 John Wiley & Sons, Ltd. ISBN: 0-471-49926-9. pg. 59.

[xlviii] Gasteiger, H. A., Gu, W., Makharia, R., Mathias, M. F., and Sompalli, B. "Beginning-of-life MEA performance – Efficiency loss contributions." *Handbook of Fuel Cells: Fuel Cell Technology and Applications.* Edited by Wolf Vielstich, Arnold Lamm, and Hubert A. Gasteiger. Volume 3: *Fuel Cell Technology and Applications, Part 1.* © 2003 John Wiley & Sons Ltd. pg. 596-608.

[xlix] Gattrell, M. and MacDougall, B. "Reaction mechanisms of the $O_2$ reduction/evolution reaction." *Handbook of Fuel Cells – Fundamentals, Technology and Applications*, Edited by Wolf Vielstich, Hubert A. Gasteiger, Arnold Lamm. Volume 2: *Electrocatalysis*. © 2003 John Wiley & Sons, Ltd. ISBN: 0-471-49926-9. pg. 444-445.

[l] Bockris & Srinivasan. Pg. 137-139.

[li] Thompsett, D. "Pt alloys as oxygen reduction catalysts." *Handbook of Fuel Cells: Fuel Cell Technology and Applications.* Edited by Wolf Vielstich, Arnold Lamm, and Hubert A. Gasteiger. Volume 3: *Fuel Cell Technology and Applications, Part 1.* © 2003 John Wiley & Sons Ltd. pg. 468.

[lii] Mukerjee and S. Srinivasan. "$O_2$ reduction and structure-related parameters for supported catalysts." Pg. 506.

[liii] Xiong, L. and Manthiram, A. "Effect of Atomic Ordering on the Catalytic Activity of Carbon Supported PtM (M = Fe, Co, Ni, and Cu) Alloys fro Oxygen Reduction in PEMFCs." *J. Electrochemical Society*, 2005, vol. 152, no. 4, p. A697-A703.

[liv] Lima, Fabio H. B., Giz, M. Janete and Ticianelli, Edson A.. *J. Braz. Chem. Soc.*, May/June 2005, vol. 16, no. 3a, p. 328-336. ISSN 0103-5053.

[lv] C. Sanchez and E. Leiva. "Catalysis by UPD metals." Pg. 59.

[lvi] T. E. Mallouk and E. S. Smotkin. "Combinatorial catalyst development methods." *Handbook of Fuel Cells – Fundamentals, Technology and Applications*, Edited by Wolf Vielstich, Hubert A. Gasteiger, Arnold Lamm. Volume 2: *Electrocatalysis*. © 2003 John Wiley & Sons, Ltd. ISBN: 0-471-49926-9. pg. Pg. 341.
[lvii] Lima, Fabio H. B., Giz, M. Janete and Ticianelli, Edson A.
[lviii] Bockris & Srinivasan. pg. 330-332.
[lix] Bockris & Srinivasan. pg. 330.
[lx] E. Leiva and C. Sanchez. "Theoretical aspects of some prototypical fuel cell reactions." *Handbook of Fuel Cells – Fundamentals, Technology and Applications*, Edited by Wolf Vielstich, Hubert A. Gasteiger, Arnold Lamm. Volume 2: *Electrocatalysis*. © 2003 John Wiley & Sons, Ltd. ISBN: 0-471-49926-9. pg. 128.
[lxi] Bockris & Srinivasan. pg. 332.
[lxii] M. Gattrell and B. MacDougall. "Reaction mechanisms of the $O_2$ reduction/evolution reaction." pg. 456.
[lxiii] U. A. Paulus, T. J. Schmidt and H. A. Gasteiger. "Poisons for the $O_2$ reduction reaction". *Handbook of Fuel Cells – Fundamentals, Technology and Applications*, Edited by Wolf Vielstich, Hubert A. Gasteiger, Arnold Lamm. Volume 2: *Electrocatalysis*. © 2003 John Wiley & Sons, Ltd. ISBN: 0-471-49926-9. pg. 555.
[lxiv] M. Gattrell and B. MacDougall. "Reaction mechanisms of the $O_2$ reduction/evolution reaction." pg. 479.
[lxv] *MITS Pro Help*.
[lxvi] Hamnett, A. "The components of an electrochemical cell." pg. 6.
[lxvii] Bockris & Srinivasan. Pg. 197.
[lxviii]Barbir, Frano.
[lxix] Barbir, Frano.
[lxx] Barbir, Frano.
[lxxi] Barbir, Frano.
[lxxii] Bockris & Srinivasan. Pg. 325.